A novel form of glycolytic metabolism-dependent cardioprotection revealed by PKCα and β inhibition

Sean Brennan[1,2], Shen Chen[1], Samir Makwana[1], Christopher A. Martin[1], Mark W. Sims[1], [3,4]Asma S.A. Alonazi, [3]Jonathan M Willets, Iain B. Squire[1,5], Richard D. Rainbow[1,2].

[1]Department of Cardiovascular Sciences, University of Leicester, Glenfield General Hospital, Leicester, UK,

[2]Department of Molecular and Clinical Pharmacology, Institute of Translational Medicine, University of Liverpool, Liverpool, UK

[3]Department of Molecular and Cellular Biology, University of Leicester, Leicester, UK

[4]Department of Pharmacology and Toxicology, Pharmacy College, King Saud University, Riyadh, KSA

[5]Leicester NIHR Biomedical Research Centre, Glenfield General Hospital, Leicester, UK

Correspondence

Dr R D Rainbow, Department of Molecular and Clinical Pharmacology, Institute of Translational Medicine, University of Liverpool, Liverpool, UK, email: richard.rainbow@liverpool.ac.uk

Abstract

Background: Hyperglycaemia has a powerful association with adverse prognosis for patients with acute coronary syndromes (ACS). Previous work shows high glucose prevents ischaemic preconditioning and causes electrical and mechanical disruption via PKCα/β activation.

The aims of this study were to: 1) determine whether the adverse clinical association of hyperglycaemia in ACS can be replicated in preclinical cellular models of ACS. 2) Ascertain the importance of PKCα/β activation to the deleterious effect of glucose.

Methods: Freshly isolated rat, guinea pig or rabbit cardiomyocytes were exposed to simulated ischaemia after incubation in the presence of normal (5mM) or high (20mM) glucose in the absence or presence of small molecule or tat-peptide-linked PKCαβ inhibitors. In each of the 4 conditions, the following hallmarks of cardioprotection were recorded using electrophysiology or fluorescent imaging: cardiomyocyte contraction & survival, action potential stability & time to failure, intracellular calcium & ATP, mitochondrial depolarisation, ischaemia-sensitive leak current and time to $K_{ir}6.2$ opening.

Results: High glucose alone resulted in decreased cardiomyocyte contraction and survival, however, imparted cardioprotection in the presence of PKCα/β inhibitors. This cardioprotective phenotype displayed improvements in all measured parameters and decreased myocardium damage during whole heart coronary ligation experiments.

Conclusions: High glucose is deleterious to cellular and whole-heart models of simulated ischaemia, in keeping with the clinical association of hyperglycaemia with adverse outcome in ACS. PKCαβ inhibition revealed high glucose to show a cardioprotective phenotype in this setting. This study suggests the potential for therapeutic application of PKCαβ inhibition in ACS associated with hyperglycaemia.

Introduction

Acute coronary syndromes (ACS) encompass a spectrum of acute myocardial ischaemia and injury, ranging from unstable angina and non-ST-segment elevation myocardial infarction, to ST-segment elevation myocardial infarction (Yiadom, 2011). Current ACS therapies focus on restoring reperfusion to the ischaemic territory to salvage viable myocardium and prevent artery re-occlusion, and so improve the clinical outcome (Niccoli *et al.*, 2015). Somewhat paradoxically, coronary artery reperfusion, while relieving ischaemia, has itself been associated with myocardial damage, an event which has been termed 'myocardial reperfusion injury' (Niccoli *et al.*, 2015). Development of adjunctive therapies to reduce ischaemia and reperfusion injury have gained increasing attention, partly due to the inevitable logistical delay in restoring reperfusion in ACS (Lassen *et al.*, 2013). While experimental evidence suggests that a number of pharmacological stimuli may be beneficial in reducing reperfusion injury, translation into clinical application has so far proved challenging (Schmidt *et al.*, 2014).

Acute hyperglycaemia, acute elevations in blood glucose often termed 'stress hyperglycaemia', is common in the setting of ACS, and is associated with adverse outcome, irrespective of a prior diagnosis of diabetes mellitus (Squire *et al.*, 2010; Steg *et al.*, 2012; Fujino *et al.*, 2014). Even minor elevations of blood glucose (above 8.2mmol/l) have been associated with adverse impact on outcome after ACS (Squire *et al.*, 2010; Gardner *et al.*, 2015; Al Jumaily *et al.*, 2015). The American Heart Association (AHA) (O'Gara *et al.*, 2013), the National Institute for Health and Care Excellence (NICE) (Corbett, 2012) and the European Society of Cardiology (Steg *et al.*, 2012) all acknowledge the importance of managing hyperglycaemia in patients with ACS. Despite this, hyperglycaemia remains underappreciated as a risk factor in ACS and is frequently untreated (Kosiborod & Deedwania, 2009). The AHA stated that more research is necessary to enhance the understanding of the relationship between elevated glucose and adverse outcomes, plus whether treatment of hyperglycaemia improves outcomes (Deedwania *et al.*, 2008).

The molecular mechanism of damage to the myocardium during ACS is a controversial area of the literature, however it is commonly acknowledged that disruption of mitochondrial function is a key

component. Overload of $[Ca^{2+}]_i$, dissipation of the mitochondrial membrane potential and low levels of ATP are proposed to lead to necrotic or apoptotic death via formation of the mitochondrial permeability transition pore (Nesci, 2018; Briston *et al.*, 2019). This is proposed to lead to an efflux of reactive oxygen species (ROS) and cytochrome C into the cytoplasm, driving further release of ROS from the matrix of the mitochondrion, which propagates cellular damage across the microenvironment and initiates apoptotic signalling in the neighbouring cells (Penna *et al.*, 2009). Hyperglycaemia has been suggested to exacerbate this injury by promoting mitochondrial membrane depolarisation in H9C2 cells (Kumar *et al.*, 2012), whilst Su *et al*. suggested that there was an increase ROS generation, increased caspase activity and infarct area in the hyperglycaemic myocardium (Su *et al.*, 2013).

Ex vivo experiments have demonstrated the direct toxicity of elevated glucose concentrations to whole heart and isolated cardiomyocytes preparations. Acute hyperglycaemia to whole rat hearts prior to experimental ischaemia and reperfusion caused myocardial oxidative stress, apoptosis and cardiac contractile dysfunction (Mapanga *et al.*, 2014). Recently, we reported the deleterious effects of elevated glucose to freshly isolated cardiomyocytes in a non-ischaemic setting (Sims *et al.*, 2014). In short, elevated glucose caused electrical instability, disruption of Ca^{2+} homeostasis and decreased cardiomyocyte survival. These deleterious effects of elevated glucose were all attenuated by various protein kinase C α/β (PKCα/β) inhibitors.

This study aimed to determine whether elevated glucose has adverse effects on cardiomyocyte survival in cellular and whole heart models of ACS, and whether PKCα/β inhibition could attenuate any such effect. We report a mechanism that may contribute to the clinically demonstrated deleterious effects of high glucose in patients with ACS. We show that PKCα/β inhibition attenuates the deleterious effects of elevated glucose and reveals a metabolism-dependent cardioprotection to freshly isolated cardiomyocytes in against simulated ischaemia and whole-heart left coronary artery ligation. These data suggest that PKCα/β inhibition as a potential therapeutic target in ACS.

Materials and methods

Ethical Approval:

Adult male Wistar rats (300–400 g, 12 – 14 weeks old, n = 102, bred in-house at the University of Leicester) or Dunkin-Hartley guinea pigs (up to 500 g, 12 – 14 weeks old, n = 8, purchased from Harlan UK), were killed by concussion and cervical dislocation. Rats and guinea pigs were maintained in 1800 cm^2 Tecniplast cages, using BED01/8 Dates and corn cob for bedding, housed in IVC caging (SPF free). The number of cage companions for the animals of 300–400 g is 5 based on a calculation of 350 cm^2 being required for each rat or guinea pig of that size. Experiments were also conducted on cardiomyocytes isolated from New Zealand white rabbit hearts (2.0–3.0 kg, 10 – 13 weeks old, n = 6, purchased from Envigo). Briefly, animals were pre-medicated with ketamine (Ketaset, 10 mg/kg, Fort Dodge, UK), medetomidine hydrochloride (Sedator, 0.2 mg/kg, Dechra, UK) and butorphanol (Torbugesic, 0.05 mg/kg, Fort Dodge, UK) (i.m.). Following stable sedation, animals were sacrificed with an overdose of sodium pentobarbitone (Euthetal, Rhone Merieux, UK; 111 mg/kg body weight, i.v.) containing Heparin (1000 IU, Multiparin, UK) delivered via the marginal ear vein. The care and sacrifice of the animals conformed to the requirements of the U.K. Animals (Scientific Procedures) Act 1986 (2012 amendment).

Solutions:

The normal Tyrode's (NT) solution contained (in mM): 135 NaCl, 5 KCl, 0.33 NaH_2PO_4, 5 Na-pyruvate, 10 4-(2-hydroxyethyl)-1-piperazineethanesulphonic acid (HEPES), 1 $MgCl_2$ and 2 $CaCl_2$ (pH 7.4 with NaOH). Glucose was added to the solution as indicated in the text. Nominally Ca^{2+} -free Tyrode's solution used during cardiomyocyte isolation was as outlined above with no added Ca^{2+}. Substrate-free 2 mM Ca^{2+} Tyrode's (SFT) contained, in mM, 140 NaCl, 5 KCl, 0.33 NaH_2PO_4, 10 HEPES, 10 Sucrose 1 $MgCl_2$ and 2 mM $CaCl_2$ (pH 7.4).

For all experiments, NT with 5 mM glucose was considered as the control glucose concentration as it is within the physiological fasting range (NICE guideline PH38). Clinically, hyperglycaemia is defined as a blood glucose concentration above 11 mM (NICE guideline [CG130]). To investigate the effects of raised glucose, NT solutions containing 10, 15, 20 and 30 mM glucose were used, and mannitol was used to ensure all Tyrode's solutions were osmotically balanced. This range of glucose, although well

into the pathophysiological range, has been shown to be relevant to real clinical scenarios during MI (Squire *et al.*, 2010). To ensure that the observations were due to changes in glucose a number of control experiments were conducted to control for osmolality. The pipette solution for whole-cell recording contained (in mM): 30 KOH, 5 EGTA, 110 KCl, 10 HEPES, 1 $MgCl_2$, 0.61 $CaCl_2$, 1 ATP, 0.1 ADP and 0.1 GTP, (pH 7.2 with KOH). For cell-attached patch recording, the solution contained (in mM): 140 KCl, 10 HEPES, 0.5 $MgCl_2$ and 1 $CaCl_2$ (pH 7.4 with KOH).

The protocol for isolation of ventricular cardiomyocyte was as described previously (Hudman & Standen, 2004; Rainbow *et al.*, 2005; Sims *et al.*, 2014; Brennan *et al.*, 2015). For rat and guinea pig cardiomyocytes isolations, the heart was rapidly excised, temporarily placed into cold, nominally Ca^{2+}-free NT solution to stop contraction, and quickly cannulated via the aorta on a Langendorff type apparatus. Warmed Ca^{2+}-free NT (37 °C) was then perfused through the heart in a retrograde fashion for 6 min to clear residual blood. Following this, the solution was exchanged for a Ca^{2+}-free NT with enzyme mix (0.5 mg.ml-1 collagenase type II (Worthington, USA), 1.66 $mg.ml^{-1}$ BSA from factor V albumin (Sigma-Aldrich, UK) and 0.6 $mg.ml^{-1}$ protease (type XIV 15 % Ca^{2+}; Sigma-Aldrich, UK) for 8 – 15 min. The presence of rod shaped cardiomyocytes in the perfusate was used as an indication of digestion being complete. The solution was then exchanged for a 2 mM Ca^{2+} NT solution to inhibit the enzyme mix, the heart cut down and cardiomyocytes mechanically dispersed from the tissue in a shaking water bath at 37°C. Typically this method yielded 70 – 90 % rod-shaped cardiomyocytes, which were stored in NT solution at room temperature and used within 8 hr of isolating. Ischaemic preconditioning (IPC) was imparted to cardiomyocytes using a protocol involving 3 cycles of halted perfusion followed by re-perfusion (Rodrigo & Samani, 2008; Sims *et al.*, 2014; Brennan *et al.*, 2015). IPC cardiomyocytes were used up to 6 hr after isolation.

For rabbit cardiomyoycte isolaton, the hearts were rapidly excised, placed into ice cold Ca^{2+}-free Tyrode's solution and then retrogradely perfused through the ascending aorta in conditions of constant flow Langendorff mode (40 ml/min). An enzyme solution, containing 1mg/ml Type II collagenase (Worthington), 0.66mg/ml Protease and 1.66 mg/ml Bovine Serum Albumin (essentially fatty acid free), was perfused for 8 minutes. Following this, the heart was perfused with NT for 3 minutes prior

to cutting the left ventricle away from the remaining tissue. Cells were mechanically dispersed as described for rat and guinea pig cardiomyocytes and used within 8 hr.

Clinical data

The clinical data presented in this paper were gathered during routine care of patients admitted with a diagnosis of acute STE segment elevation myocardial infarction (STEMI) as previouly been reported (Squire *et al.*, 2010). The diagnosis required (i) EKG evidence of dynamic ST segment elevation together with (ii) appropriate symptoms and (iii) increase in serum levels of CK to greater than twice the upper limit of the laboratory reference range (ie >400 IU/L). Troponin concentrations were not available for the full study period. Although predating the Myocardial Ischaemia National Audit Project, our database is that used by our hospital for this purpose. In this context, data collection does not require individual patient consent. The project was approved by the local research ethics committee. Data are from consecutive admissions (1 January 1993 to 31 December 2005) to the coronary care unit of a large teaching hospital (Leicester Royal Infirmary). The blood glucose concentration used was that first recorded for the index admission, assayed as part of routine investigations.

Simulated ischaemia and reperfusion models:

Cardiomyocyte contraction and cell death was investigated using two different metabolic poisons. 1) Substrate-free metabolic inhibition Tyrode's solution (SFT-MI; contained 2 mM cyanide to inhibit oxidative phosphorylation and 1 mM iodoacetic acid to inhibit GAPDH) (Rainbow *et al.*, 2004; Hudman & Standen, 2004; Sims *et al.*, 2014; Brennan *et al.*, 2015). 2) Ischaemic buffer contained in mmol/L, 108 NaCl, 16 KCl, 0.33 NaH_2PO_4, 10 PIPES, 20 deoxyglucose, 20 Na-lactate, 1 $MgCl_2$, 2 $CaCl_2$, and 0.2 2,4-dinitrophenol (DNP), pH 6.8 with NaOH) (Brennan *et al.*, 2015). Cardiomyocytes were perfused at a rate of 5 $ml.min^{-1}$ at 32°C, stimulated to contract via 1 Hz electric field stimulation (EFS) and contractile function observed via a JVC CCTV camera and recorded to DVD. The experimental protocol is shown in each figure.

Patch Clamp Electrophysiology:

Conventional patch pipettes were used in the whole-cell configuration in either voltage-clamp or current-clamp mode to record metabolically sensitive "leak" current or action potentials, respectively. Recordings were made from isolated cardiomyocytes using an Axopatch 200B amplifier, digitized using a Digidata 1440 and recorded and analysed using pCLAMP 10.7 software (RRID:SCR_011323, Axon instruments, Scientifica, Uckfield UK).

Fluorescent imaging:

Cardiomyocytes were loaded with either Fura-2-AM (excitation 340:380 nm, emission collected >520 nm), Magnesium Green (excitation 480 nm, emission collected >520 nM) or Tetramethylrhodamine methyl ester (TMRM) (excitation 546 nm, emission collected >560 nM) for 10-20 min to measure $[Ca^{2+}]_i$, intracellular [ATP] or mitochondrial membrane potential, respectively. Fluorescence was excited using a monochromator (PTI, Birmingham, NJ, USA) at 0.2 Hz for 40 ms to minimise photobleaching. Emissions were captured using a Cascade 512B CCD camera (Photometrics, Tuscan, AZ, USA) and processed using EasyRatioPro software (PTI, Birmingham, NJ, USA).

Langendorff-perfused heart and coronary artery ligation.

The heart was allowed to stabilize for 1 hr. The left anterior descending coronary artery was then ligated (40 min) to cause ischaemia by using 5-0 USP braided silk suture and two pipette tips to form a reversible knot around the artery (Figure 15A, second picture from left). The knot was then removed to start the 3-hr reperfusion phase with the suture remaining in place to allow for re-ligation (Figure 14A, third picture from left). During all phases temperature was carefully kept at 37°C by submerging the heart in Tyrode's solution using a heated water jacket. Evans Blue dye (1% in Tyrode's solution) and 2,3,5-triphenyltetrazolium chloride (Sigma Aldrich) were used to identify area at risk (AAR) and infarcted area (IA), respectively. To determine the AAR and IA, each slice was scanned on both sides and weighed. AAR and IA were calculated for each of the slices from the heart using ImageJ. The AAR, IA and unaffected area sizes from ImageJ (RRID:SCR_003070) were then used to calculate the percentage infarct of the AAR by weight.

Western blotting.

Hearts from an adult male Wistar rats (300 – 400 g) were rapidly excised and perfused for 30 min at 37 °C on a Langendorff system with 5 mM glucose, 20 mM glucose or 5 mM glucose Tyrode's solution with 1 μM PMA. Hearts were then snap frozen in liquid nitrogen and stored at -80 °C. When required hearts were chopped and added to ice-cold lysis buffer (Tris-HCl pH 7.4, 20 mM; 1% (v/v) Triton X-100, NaCl, 137 mM; EDTA, 2 mM, sodium orthovanidate; 1 mM; phenylmethanesulphonylfluoride, 500 μM; leupeptin, 0.1 mg/mL; benzamidine, 0.2 mg/mL; pepstatin, 0.1 mg/mL). Tissues were then homogenisation on ice using a Polytron PT210 homogeniser (Kinematica, Basel, Switzerland), prior to centrifugation at 1000 rpm to remove nuclear material. The resulting supernatant was removed and subjected to a further centrifugation step at 14,000 rpm to separate the cytosolic and membrane fractions. Once the cytosolic fraction was removed, the membrane pellet was re-suspended in lysis buffer and the protein content of all fractions determined by the Bradford method (Bradford, 1976). Samples were diluted to 1mg/ml by the addition of 2x sample buffer (250 mM Tris-HCl, pH 6.8, 0.01% bromophenol blue (w/v), 2% SDS (w/v), 40% (v/v) glycerol and 50 mM dithiothreitol). Samples were then boiled for 5 min before separation of 40 μg of each sample on 10% SDS-PAGE gels, transferred to nitrocellulose and blocked using standard Western blotting techniques. Phospho PKCα (ab76016; 1:50,000) was detected using specific anti-rabbit antibodies (Abcam, Cambridge, UK), whilst total PKCα or PKCε (both 1:1000) were simultaneously detected using specific anti-mouse antibodies (BD Biosciences, Wokingham, UK). After incubation with secondary antibodies anti-rabbit IgG (H+L) DyLight 680-conjugate and anti-mouse IgG (H+L) DyLight 800-conjugate (Cell Signaling Technology), proteins were detected with infrared fluorescence using the Odyssey CLx imaging system (LI-COR, Cambridge, UK). Protein expression was quantified by densitometry using Image J (version 1.51, National Institutes of Health, Bethesda, MD) (RRID:SCR_003070). G protein coupled receptor kinase 2 expression was also determined using a mouse anti-GRK2 antibody (sc-13143; 1:1000; Santa Cruz, Biotech., CA, USA) using similar Western blotting techniques as described above.

PKC inhibition

Tat-linked PKC inhibitor peptides were used at a concentration of 100 nM as described previously (Rainbow *et al.*, 2009; Sims *et al.*, 2014; Brennan *et al.*, 2015). Isolated cardiomyocytes were pre-

incubated for 10 min with Tat-linked peptides, or the Tat-peptide with no linked peptides as a control, prior to experimentation. PKCα and β were also pharmacologically inhibited in isolated cardiomyocytes using Gö 6976 (300 nM: Tocris, Bristol, UK) and LY 379196 (300 nM; a kind gift from Eli Lilly, Indianapolis, USA). Tat-Linked peptides were soluble in water, however other drugs required to be diluted from stock solutions in DMSO. The maximum DMSO concentration was 0.1%. Equivalent volumes of vehicle (DMSO) had no effect on cardiomyocyte function in these experiments.

Statistical analyses:

All patch clamp data were analysed using pCLAMP10.7 (RRID:SCR_011323) and Microsoft Excel 2016 (RRID:SCR_016137) software. Calcium, MgGreen and TMRM imaging data were analysed using WinFluor4.0.2 (Dr John Dempster, University of Strathclyde). Contractile function data were analysed in Microsoft Excel. All figures were made in Graphpad Prism 7 (RRID:SCR_002798) and statistical analysis was performed in Prism 7 as indicated in the text.

Results

Elevated glucose is deleterious to cardiomyocyte function and viability during simulated ischaemia.

Acute hyperglycaemia, which may result from stress, is common among AMI patients, irrespective of prior diabetes status, and is associated with poor outcome. Figure 1A&B show the distribution of blood glucose concentration at the time of admission from 3854 non-diabetic or diabetic AMI patients. A large proportion (>48%) of patients without a prior diagnosis of diabetes have a blood glucose of >8 mM. Previous reports have shown that, irrespective of diabetic status, a blood glucose concentration of >8 mM is associated with poor outcome for AMI patients (Squire *et al.*, 2010; Timmer *et al.*, 2011; Steg *et al.*, 2012; Fujino *et al.*, 2014; Gardner *et al.*, 2015; Al Jumaily *et al.*, 2015). From these data, 20 mM glucose was deemed sufficient to investigate, using cellular and whole-tissue AMI models, the damage caused by acute glucose and the therapeutic potential of mechanisms that may

remove any glucose-induced deleterious effect. In this study, the effects of acutely elevated glucose at the time of AMI was investigated using tissues from non-diabetic animals.

We previously described the deleterious effects of elevated glucose to freshly isolated cardiomyocytes in non-ischemic conditions (Sims *et al.*, 2014). To determine whether high glucose also impacts the viability, or survival, of cardiomyocytes during and after simulated ischaemia and reperfusion, cardiomyocytes were exposed to a range of glucose concentrations prior to, and following, simulated ischaemia. In accordance with our previous findings (Sims *et al.*, 2014), elevated glucose significantly reduced the proportion of rod-shaped cardiomyocytes maintaining contractile function at the beginning of the experiment (Figure 1C). Using two different simulated ischaemia protocols, raised glucose, in a concentration-dependent manner, decreased the percentage of cardiomyocyte contractile recovery and cell survival in both metabolic poisons used (Figure 1, SFT-MI & Figure 2, Ischaemic Buffer (Brennan *et al.*, 2015)). The ischaemic buffer also lead to arrhythmic contractions upon reperfusion, presumably due to the buffer's high potassium content, which increased in frequency in 20G (Figure 2B and F). These findings were not confined to rat cardiomyocytes; observations were similar using freshly isolated guinea pig (Figure 3A-C) and rabbit (Figure 4A-C) cardiomyocytes. Combined these data suggest, in accordance with the clinical literature (Squire *et al.*, 2010) and our previous work (Sims *et al.*, 2014), that elevated glucose is deleterious to cardiomyocyte function and viability after simulated ischaemia.

Elevated glucose is cardioprotective in the presence of PKCα/β inhibition during simulated ischaemia

Our previous publication demonstrated that the deleterious effects of high glucose on cardiomyocytes in a non-ischemic setting were PKCα/β dependent (Sims *et al.*, 2014). The aim of the present study was to ascertain whether PKCα/β activation was also responsible for the deleterious outcome of high glucose during simulated ischaemia. PKCα/β were inhibited using both pharmacological (300nM Gö6976 or LY379196) and peptide (Tat-PKC20-28, Tat-PKCα and Tat-

PKCβ) inhibitors. The proportion of rod-shaped cardiomyocytes contracting at the beginning of the experiment in 20G was increased by each PKCα/β inhibitor used, comparable to our previous findings (Sims *et al.*, 2014) (Figure 5A). The contractile recovery and survival of cardiomyocytes in 20G at the end of the simulated ischaemia protocol was enhanced by pre-incubation with any PKCα/β inhibitor (Figure 5B-C, $p<0.001$). Notably, activation of the well-established effector of cardioprotection, PKCε, was not responsible for the cardioprotection observed as the Tat-PKCε inhibitor did not abolish the cardioprotective effect. Furthermore, when using the ischaemic buffer protocol, Gö6976 also revealed a cardioprotective effect of high glucose in experiments and caused a significant decrease in arrhythmic contractions seen in 5G or 20G alone (Figure 2). Gö6976 also revealed a glucose-dependent protection in freshly isolated guinea pig (Figure 3D-F) and rabbit (Figure 4D-F) cardiomyocytes. These data suggest that PKCα/β inhibition prevents the deleterious effects associated with elevated glucose, and additionally reveals a cardioprotective effect of high glucose during simulated ischaemia.

Elevated glucose causes an increase in phosphorylated PKCα translocation to the membrane.

To determine whether glucose was able to active PKC, western blotting of total and phospho-PKCα in whole heart lysates was carried following 30 min of pre-treatment with 5 mM, 20 mM and 5 mM glucose with 1 μM PMA. In both 20 mM glucose and PMA-treated hearts, the phosphorylated PKCα was increased compared to 5 mM glucose control hearts (Figure 6). PKCε was not translocated to the membrane fraction in 20 mM glucose, suggesting it was not activated by elevated glucose. GRK2 is a cytosolic protein which is recruited to the plasma membrane upon ligand activation of G protein-coupled receptors. Under resting conditions, most of the kinase is found in the cytoplasm, thus, to confirm successful fractionation, the relative distribution of GRK2 was examined. Reassuringly, strong GRK2 expression was observed in all the cytosolic fractions with only minimal levels detected in the membrane fractions. In addition, glucose treatment did not recruit GRK2 to the membrane, further highlighting the glucose-dependent selective recruitment of PKCα.

Both deleterious and cardioprotective effects of elevated glucose are mediated via glycolytic metabolism

To determine whether the effects of 20G were dependent on glycolytic metabolism, cardiomyocyte function was investigated in the presence of the non-metabolised enantiomer of glucose, L-glucose, which acts as a competitive glycolytic metabolic inhibitor. L-glucose (10mM) attenuated both the deleterious (Figure 7A; $p<0.05$) and the cardioprotective (+300nM Gö6976; Figure 3A&B; $p<0.001$) effect of 20G on contractile recovery and cell survival. These results imply that competitive inhibition of glycolytic metabolism reduces both the deleterious and the revealed cardioprotective effect (+PKCα/β inhibition) of 20G. A role for glycolytic metabolism was further supported by experiments altering the amount of pyruvate or substituting fructose for glucose. In a concentration-dependent manner, both metabolized sugars, glucose and fructose, caused decreased contractile recovery and cell survival. However, both sugars elicited a concentration-dependent cardiomyocyte protection upon PKCα/β inhibition with Gö6976 (Figure 7C-F). Similar results were obtained whether the solutions used were osmotically balanced by the non-metabolized sugar mannitol or in the absence of any osmotic balance (Figure 7G-I), suggesting changes in osmolality were not responsible for the observations. Collectively, these data suggest that both the harmful effects caused by 20G, and the cardioprotection from 20G revealed by PKCα/β inhibition during simulated ischaemia are dependent on glycolytic metabolism.

In the presence of 20G, Gö6976 delays time to action potential failure during simulated ischaemia and attenuates variation of APD_{90}.

We have previously shown that 20G causes perturbation in electrical signalling and disruption of intracellular calcium homeostasis (Sims *et al.*, 2014). Fluorescent imaging and electrophysiology were employed to establish whether the protection against simulated ischaemia by 20G and the PKCα/β inhibitor Gö6976 was caused by changes in electrical excitability.

Using electrophysiology to measure action potentials, during simulated ischaemia, cardiomyocytes perfused with 20G, but not with 5G (Figure 8A), displayed early after depolarisations (EADs), which were prevented by Gö6976 (Figure 8B). The EAD caused by 20G resulted in variation in the action potential duration to 90% repolarized (APD_{90}) before and during simulated ischaemia; this was prevented by Gö6976 (Figure 8C). The extent of APD instability can be visualised by means of the Poincaré plot of the mean APD_{90} vs mean APD_{90+1}. In such a plot, identical action potentials project to a single point. Figure 4 shows that in all conditions other than 20G without Gö6976, APD_{90} was stable during SFT-MI. These data suggest that the EADs and APD variation caused by 20G are dependent on PKCα/β activation.

Prolonged perfusion with SFT-MI resulted in cardiomyocyte action potential failure (Figure 8Ci-ii); however, this was delayed by Gö6976 with 20G (Figure 8E; $p<0.001$). As cardioprotective stimuli delay the time to action potential failure (Brennan *et al.*, 2015), these data suggest PKCα/β inhibition in high glucose is cardioprotective .

Cardiomyocytes in the presence of elevated glucose and PKCα/β inhibition display the classical hallmarks of a cardioprotective phenotype.

Our previous work has shown that well-characterised cardioprotective stimuli (i.e. Adenosine and ischaemic preconditioning) preserve efficient calcium handling, intracellular ATP and mitochondrial function which, in turn, delays the activation of a metabolic sensitive leak current caused by the opening of sarcolemmal ATP-sensitive (Kir6.2/SUR2A) potassium (K_{ATP}) channel (Brennan *et al.*, 2015). A combination of fluorescent imaging and electrophysiology was used to determine whether these hallmarks of a cardioprotective phenotype were observed in conditions of elevated glucose with PKCα/β inhibited.

The emitted fluorescence of the Fura-2, Mg-Green or TMRM loaded cardiomyocytes increased during the simulated ischaemia protocol in all experimental conditions (Figure 9 and 10), indicative of increased intracellular calcium, decreased ATP and mitochondrial depolarisation, respectively. In the absence of Gö6976, the Fura-2 ratio and Mg Green fluorescence increase at the end of the protocol was

greater in cardiomyocytes exposed to 20G compared to 5G. Gö6976, however, attenuated the Fura-2 ratio and TMRM fluorescence increase in cardiomyocytes exposed to 20G (Figure 9 and 10). The preservation of intracellular ATP can also explain the delayed opening of the sarcolemmal ATP-sensitive (Kir6.2/SUR2A) potassium (K_{ATP}) channel and metabolic sensitive leak current in 20G with Gö6976 (Figure 11). These data suggest that PKCα/β inhibition reveals a protective effect of 20G, which display all the hallmarks of a cardioprotective phenotype usually associated with established cardioprotective stimuli such as adenosine (Brennan *et al.*, 2015).

Gö6976 and LY379196 applied at any phase of simulated ischaemia protects cardiomyocytes in the presence of elevated glucose.

Pre-incubation of PKCα/β inhibitors prior to the simulated ischaemia protocol revealed a cardioprotective effect of 20G (Figure 5). To consider the potential clinical application of PKCα/β inhibition in treatment of ACS, Gö6976 (Figure 12A-C) or LY379196 (Figure 12D&F) were applied at the start of either the simulated ischaemia or reperfusion phase to closely mimic the likely therapeutic scenario. In the presence of 20G, either PKCα/β inhibitor increased cardiomyocyte contractile recovery and survival when applied during SFT-MI or at reperfusion (Figure 12B-F, $p<0.001$). Furthermore, when glucose was only elevated at reperfusion, to simulate stress-induced hyperglycaemia, both drugs improved contractile recovery and survival (Figure 12, $p<0.001$).

Gö6976 with high glucose imparts cardioprotection during whole heart coronary ligation

Left anterior descending (LAD) coronary artery ligation to whole hearts perfused, on an *ex vivo* Langendorff preparation, was used to determine whether PKCα/β inhibition could impart protection to whole tissue. As expected, perfusion with 20G lead to more damage to the myocardium compared to 5G control ($p<0.001$), however, the presence of Gö6976 with 20G decreased the damage to the myocardium (Figure 14, $p<0.05$).

Discussion

The association between elevated blood glucose at admission with ACS and subsequent adverse prognosis is well established (Squire *et al.*, 2010; Fujino *et al.*, 2014; Gardner *et al.*, 2015; Al Jumaily *et al.*, 2015). While national and international guidelines suggest consideration should be given to active management of elevated glucose in ACS, only a minority of cases receive such treatment (Kosiborod *et al.*, 2005; Weston *et al.*, 2007; Steg *et al.*, 2012; Corbett, 2012; O'Gara *et al.*, 2013). This apparent clinical inertia is likely to stem at least in part from the lack of a clear mechanism by which elevated glucose might be directly harmful to cardiomyocytes. The current study provides such evidence of such a mechanism.

We previously reported toxicity from elevated glucose to isolated cardiomyocytes (Sims *et al.*, 2014) and augmented agonist-induced vasoconstriction vascular smooth muscle (Jackson *et al.*, 2016), via PKCα/β activation. The current report shows that elevated glucose exerted toxicity to isolated cardiomyocytes in simulated ischaemia via PKCα/β activation. Unexpectedly, we observed that not only did PKCα/β inhibition attenuate glucose-mediated cardiotoxicity, it in fact imparted protection from simulated ischaemia to cardiomyocytes in elevated glucose. Analogous results were obtained across all three species tested (rat, guinea pig and rabbit) and in either model of simulated ischaemia used. The protection displayed all the classical hallmarks of known cardioprotective stimuli, including improved calcium handling and contractile recovery (Figure 15).

Putative mechanisms for glucose-induced damage have concentrated on ROS generation, advanced glycation end products (AGES), sympathetic drive, and the potential for *de novo* DAG synthesis from a backup of glycolytic metabolites (Brownlee, 2001; Shah & Brownlee, 2016). The absolute mechanism of glucose-induced damage of the myocardium is unclear, however our findings in this study demonstrate a clear relationship between glucose, activation of PKCα/β and electrical disturbances in the myocytes. Importantly, our findings occur with *acute* not prolonged elevations of glucose. From this it is possible to at least limit the role of AGEs in the process that we observe as these are only formed following *prolonged* hyperglycaemia. Similarly, the polyol pathway is also unlikely to be part of this *acute* mechanism.

Our observations indicate a potential mechanism by which the established clinical association between acute hyperglycaemia during acute coronary artery ischaemia with adverse outcome may be mediated. Elevated extracellular glucose had clear deleterious effects on freshly isolated cardiomyocytes *ex vivo*. The similar findings on whole heart preparations confirm similar findings in prior reports (Mapanga *et al.,* 2014). These models are free from the influence of potential confounding factors seen *in vivo*, such as sympathetic nervous system and vasoconstrictor hormone activation. We suggest our findings provide evidence of a mechanism by which hyperglycaemia may be directly toxic to cardiomyocyte integrity and function in the setting of ischaemia, and suggests that the clinical association between hyperglycaemia and adverse outcome after ACS may be the result of direct toxicity rather than an epiphenomenon.

Hyperglycaemia is a known activating signal for cardiac PKC isozymes that modulate a variety of cellular events including apoptosis (Malhotra *et al.*, 2005*a*). Previous papers have shown that inhibition of PKCβI/βII, -δ (delta) (Shizukuda *et al.*, 2002) and ζ (zeta) all attenuate the hyperglycaemia apoptosis signal while ε (epsilon) inhibition has no effect, however, PKCε activation prevents hyperglycaemia-induced apoptosis (Malhotra *et al.*, 2005*b*). This study demonstrates that elevated glucose is cardioprotective in the presence of either of the small molecule (Gö6976 and LY379196) or peptide PKCα/β inhibitors. Importantly, these PKCα/β inhibitors imparted protection to cardiomyocytes when added either at the start of the simulated ischaemia or at the reperfusion phase. In all experimental protocols in this study, the cardioprotective phenotype was revealed in the presence of both high glucose and PKCα/β inhibition; neither glucose or PKCα/β inhibition used separately caused cardioprotection. Furthermore, the use of the two-way ANOVA throughout demonstrated a significant interaction between high glucose and PKCα/β inhibition. The potential importance and usefulness of such a treatment is underlined by findings demonstrating that elevated glucose ablates the cardioprotection imparted by ischemic preconditioning (IPC) and pharmacological agents (Kersten *et al.*, 1998; Yang *et al.*, 2013; Yu *et al.*, 2014; Sims *et al.*, 2014). Collectively, these reports raise the possibility that PKCα/β inhibitors may have therapeutic potential in ACS complicated by elevated blood glucose by imparting cardioprotection and attenuating the deleterious effects of elevated glucose.

Indeed, our findings suggest the potential for therapeutic elevation of blood glucose with concomitant PKCα/β inhibition. Moreover, PKCα/β inhibition may represent an alternative strategy by which to attenuate the adverse effects of hyperglycaemia in patients with ACS, in comparison to the current use of intravenous insulin; as with hyperglycaemia, hypoglycaemia is also associated with adverse outcome in ACS (Svensson *et al.*, 2005). Therefore, intrinsic cardioprotection, and exogenous cardioprotective stimuli, may be ineffective if hyperglycaemia remains untreated. PKCα/β inhibition may provide a novel therapy to confer cardioprotection, whilst preventing hypoglycaemia caused by glucose lowering interventions. In the absence of any specific PKC inhibitors currently available to clinicians, it is possible that the use of Gq-receptor blockers, such as the angiotensin receptor blocker (ARB) Losartan, could be of benefit to reduce PKC activity indirectly. A study has shown that changes in cardiomyocyte phenotype with chronic hyperglycaemia in a streptozotocin model of diabetes were ablated by co-treatment with Losartan (Alfarano *et al.*, 2011). Our own previous work demonstrated that enhanced vasoconstriction in high glucose could be attenuated by specific PKC inhibition (Jackson *et al.*, 2016). It is plausible that ARB's could be administered to indirectly reduce PKC-mediated, hyperglycaemia-induced, potentiation of vascular contractile signalling, as well as AT-II-dependent PKC activity in cardiomyocytes, at the time of ACS.

The PKCβ inhibitor, Ruboxistaurin, an LY379196 analogue, is currently in phase I/II evaluation for treatment of heart failure. Various, pre-clinical studies have suggested PKCβ inhibition as a potential therapeutic target in heart failure via several mechanisms (Ferreira *et al.*, 2011). Nevertheless, the Ruboxistaurin clinical trials demonstrate that PKCα/β inhibitors can be well tolerated, and may provide a novel therapeutic strategy in the treatment of ACS. This study adds to the growing evidence that PKCα/β inhibitors could be useful during ACS via a number of different mechanisms. PKCα promotes thrombus formation, however, mice lacking PKCα do not have a bleeding tendency suggesting PKCα as a possible antithrombotic target (Harper & Poole, 2010) while PKCα/β inhibition has also been reported to prevent elevated glucose-potentiation of agonist-induced vasoconstriction of pig coronary and human internal mammary arteries (Jackson *et al.*, 2016). Furthermore, PKCα/β inhibition could potentially be beneficial irrespective of diabetes status as inhibition of PKCβ2

overexpression reduces myocardial ischaemia/reperfusion injury in diabetic rats (Liu *et al.*, 2015). This study demonstrated that PKCα/β inhibitors with elevated glucose revealed a cardioprotective phenotype in cellular and a whole-heart model of ACS. Combined these data suggest that the therapeutic potential of PKCα/β inhibitors in ACS warrants further investigation.

Study Limitations

Our observations were performed *ex-vivo* and should not be extrapolated directly to the clinical setting without further investigation. PKCα/β activation is one mechanism by which elevated glucose may cause harm to cardiomyocytes and by inference to whole heart function in ACS. However, numerous studies have reported the deleterious effects of hyperglycaemia on the ischaemic myocardium through oxidative stress, inflammation, apoptosis, endothelial dysfunction, hypercoagulation and platelet aggregation (Ishihara, 2012).

This study investigated the effects of acute hyperglycaemia in cellular and whole heart models of ACS, using tissue from non-diabetic animals. Acute hyperglycaemia (or stress-induced hyperglycaemia) is common amongst ACS patients hospitalised irrespective of a known diabetic status (Squire *et al.*, 2010). However, the mechanisms behind myocardial damage or protection may be different in patients with, compared to those without, diabetes; an issue that will require investigation in appropriate animal models and human population. Recent findings in cardiomyocytes isolated from a streptozotocin model of hyperglycaemia suggested that there was a delay in the time to contractile failure, ATP-depletion and K_{ATP} channel activation during metabolic inhibition compared to normoglycaemia (Alfarano *et al.*, 2011). In this study, the authors suggested that this delay was cytotoxic, placing an increased workload on the heart during ischaemia, however they also report that their diabetic cardiomyocytes were able to survive the metabolic inhibition more readily. These findings of a protected state mirror our data in high glucose, however only in the presence of PKC inhibition. The authors also report differences in glycogen store levels and glycolytic enzyme activity, both being higher in the cardiac cells isolated from the diabetic animals compared to normoglycaemic. These differences in phenotype suggest adaptation to chronic hyperglycaemia and therefore highlights the

importance of considering the effects of *acute* hyperglycaemia that can be induced in patients suffering ACS.

In summary, elevated glucose during ischaemia elicits deleterious effects on isolated cardiomyocyte function and whole heart function via a mechanism dependent upon glycolytic metabolism and PKCα/β activation. However, PKCα/β inhibition allows elevated glucose to impart protection against ischaemia. PKCα/β inhibition represents a potential therapeutic target in protecting the myocardium during ACS.

Translational perspective

Here, we demonstrate a mechanism by which elevated extracellular glucose augments the toxicity of simulated ischaemia and reperfusion on isolated cardiomyocytes, via activation of protein kinase C (PKC) α and β isoenzymes. We show that PKCα/β inhibition blocks this phenomenon and reveals elevated glucose to protect cardiomyocytes from ischaemia. Acute hyperglycaemia has a powerful association with adverse prognosis for patients with acute coronary syndromes (ACS). Our findings have implications for PKCα/β inhibition as a potential therapeutic target in ACS. Selective PKCα/β inhibition may, therefore, have potential to be a therapeutic directed towards reducing myocardial injury in ACS such as myocardial infarction. Given that aggressive treatment of hyperglycaemia with current glucose lowering therapies runs the risk of cause equally damaging hypoglycaemia, PKCα/β inhibition may provide a unique alternative to remove the cardiotoxicity of acute hyperglycaemia.

Funding:

This work was supported by the van Geest Cardiovascular Research Fund, University of Leicester (SB, RDR) and the British Heart Foundation (PG/16/14/32039) (SB, RDR), and forms part of the work of the Leicester NIHR Biomedical Research Centre.

References

Alfarano C, Suffredini S, Fantappiè O, Mugelli A, Cerbai E, Manni ME & Raimondi L (2011). The effect of losartan treatment on the response of diabetic cardiomyocytes to ATP depletion. *Pharmacol Res* **63,** 225–232.

Brennan S, Jackson R, Patel M, Sims MW, Hudman D, Norman RI, Lodwick D & Rainbow RD (2015). Early opening of sarcolemmal ATP-sensitive potassium channels is not a key step in PKC-mediated cardioprotection. *J Mol Cell Cardiol* **79,** 42–53.

Briston T, Selwood DL, Szabadkai G & Duchen MR (2019). Mitochondrial Permeability Transition: A Molecular Lesion with Multiple Drug Targets. *Trends Pharmacol Sci* **40,** 50–70.

Brownlee M (2001). Biochemistry and molecular cell biology of diabetic complications. *Nature* **414,** 813–820.

Corbett SJ (2012). NICE recommendations for the management of hyperglycaemia in acute coronary syndrome. *Heart* **98,** 1189–1191.

Deedwania P, Kosiborod M, Barrett E, Ceriello A, Isley W, Mazzone T, Raskin P, American Heart Association Diabetes Committee of the Council on Nutrition PA & Metabolism (2008). Hyperglycemia and acute coronary syndrome: a scientific statement from the American Heart Association Diabetes Committee of the Council on Nutrition, Physical Activity, and Metabolism. *Circulation* **117,** 1610–1619.

Ferreira JCB, Brum PC & Mochly-Rosen D (2011). βIIPKC and εPKC isozymes as potential pharmacological targets in cardiac hypertrophy and heart failure. *J Mol Cell Cardiol* **51,** 479–484.

Fujino M, Ishihara M, Honda S, Kawakami S, Yamane T, Nagai T, Nakao K, Kanaya T, Kumasaka L, Asaumi Y, Arakawa T, Tahara Y, Nakanishi M, Noguchi T, Kusano K, Anzai T, Goto Y, Yasuda S & Ogawa H (2014). Impact of acute and chronic hyperglycemia on in-hospital outcomes of patients with acute myocardial infarction. *Am J Cardiol* **114,** 1789–1793.

Gardner LS, Nguyen-Pham S, Greenslade JH, Parsonage W, D'Emden M, Than M, Aldous S, Brown A & Cullen L (2015). Admission glycaemia and its association with acute coronary syndrome in Emergency Department patients with chest pain. *Emerg Med J* **32,** 608–612.

Harper MT & Poole AW (2010). Diverse functions of protein kinase C isoforms in platelet activation and thrombus formation. *J Thromb Haemost* **8,** 454–462.

Hudman D & Standen NB (2004). Protection from the effects of metabolic inhibition and reperfusion in contracting isolated ventricular myocytes via protein kinase C activation. *J Mol Cell Cardiol* **37,** 579–591.

Ishihara M (2012). Acute hyperglycemia in patients with acute myocardial infarction. *Circ J* **76,** 563–571.

Jackson R, Brennan S, Fielding P, Sims MW, Challiss RJAJ, Adlam D, Squire IB & Rainbow RD (2016). Distinct and complementary roles for α and β isoenzymes of PKC in mediating vasoconstrictor responses to acutely elevated glucose. *Br J Pharmacol* **173,** 870–887.

Al Jumaily T, Rose'Meyer RB, Sweeny A & Jayasinghe R (2015). Cardiac damage associated with stress hyperglycaemia and acute coronary syndrome changes according to level of presenting blood glucose. *Int J Cardiol* **196,** 16–21.

Kersten JR, Schmeling TJ, Orth KG, Pagel PS & Warltier DC (1998). Acute hyperglycemia abolishes ischemic preconditioning in vivo. *Am J Physiol* **275,** H721-5.

Kosiborod M & Deedwania P (2009). An overview of glycemic control in the coronary care unit with recommendations for clinical management. *J Diabetes Sci Technol* **3,** 1342–1351.

Kosiborod M, Rathore SS, Inzucchi SE, Masoudi FA, Wang Y, Havranek EP & Krumholz HM (2005). Admission glucose and mortality in elderly patients hospitalized with acute myocardial infarction: implications for patients with and without recognized diabetes. *Circulation* **111,** 3078–3086.

Kumar S, Kain V & Sitasawad SL (2012). High glucose-induced Ca2+ overload and oxidative stress

contribute to apoptosis of cardiac cells through mitochondrial dependent and independent pathways. *Biochim Biophys Acta* **1820,** 907–920.

Lassen JF, Bøtker HE & Terkelsen CJ (2013). Timely and optimal treatment of patients with STEMI. *Nat Rev Cardiol* **10,** 41–48.

Liu Y, Jin J, Qiao S, Lei S, Liao S, Ge Z-D, Li H, Wong GT-C, Irwin MG & Xia Z (2015). Inhibition of PKCβ2 overexpression ameliorates myocardial ischaemia/reperfusion injury in diabetic rats via restoring caveolin-3/Akt signaling. *Clin Sci (Lond)* **129,** 331–344.

Malhotra A, Begley R, Kang BPS, Rana I, Liu J, Yang G, Mochly-Rosen D & Meggs LG (2005*a*). PKC-{epsilon}-dependent survival signals in diabetic hearts. *Am J Physiol Hear Circ Physiol* **289,** H1343-50.

Malhotra A, Kang BPS, Hashmi S & Meggs LG (2005*b*). PKCepsilon inhibits the hyperglycemia-induced apoptosis signal in adult rat ventricular myocytes. *Mol Cell Biochem* **268,** 169–173.

Mapanga RF, Joseph D, Symington B, Garson K-L, Kimar C, Kelly-Laubscher R & Essop MF (2014). Detrimental effects of acute hyperglycaemia on the rat heart. *Acta Physiol (Oxf)* **210,** 546–564.

Nesci S (2018). A Lethal Channel between the ATP Synthase Monomers. *Trends Biochem Sci* **43,** 311–313.

Niccoli G, Scalone G, Lerman A & Crea F (2015). Coronary microvascular obstruction in acute myocardial infarction. *Eur Heart J*; DOI: 10.1093/eurheartj/ehv484.

O'Gara PT et al. (2013). 2013 ACCF/AHA guideline for the management of ST-elevation myocardial infarction: a report of the American College of Cardiology Foundation/American Heart Association Task Force on Practice Guidelines. *J Am Coll Cardiol* **61,** e78-140.

Penna C, Mancardi D, Rastaldo R & Pagliaro P (2009). Cardioprotection: a radical view Free radicals in pre and postconditioning. *Biochim Biophys Acta* **1787,** 781–793.

Rainbow RD, Lodwick D, Hudman D, Davies NW, Norman RI & Standen NB (2004). SUR2A C-

terminal fragments reduce KATP currents and ischaemic tolerance of rat cardiac myocytes. *J Physiol* **557,** 785–794.

Rainbow RD, Norman RI, Everitt DE, Brignell JL, Davies NW & Standen NB (2009). Endothelin-I and angiotensin II inhibit arterial voltage-gated K+ channels through different protein kinase C isoenzymes. *Cardiovasc Res* **83,** 493–500.

Rainbow RD, Norman RI, Hudman D, Davies NW & Standen NB (2005). Reduced effectiveness of HMR 1098 in blocking cardiac sarcolemmal KATP channels during metabolic stress. *J Mol Cell Cardiol* **39,** 637–646.

Rodrigo GC & Samani NJ (2008). Ischemic preconditioning of the whole heart confers protection on subsequently isolated ventricular myocytes. *Am J Physiol Heart Circ Physiol* **294,** H524-31.

Schmidt MR, Pryds K & Bøtker HE (2014). Novel adjunctive treatments of myocardial infarction. *World J Cardiol* **6,** 434–443.

Shah MS & Brownlee M (2016). Molecular and Cellular Mechanisms of Cardiovascular Disorders in Diabetes. *Circ Res* **118,** 1808–1829.

Shizukuda Y, Reyland ME & Buttrick PM (2002). Protein kinase C-delta modulates apoptosis induced by hyperglycemia in adult ventricular myocytes. *Am J Physiol Hear Circ Physiol* **282,** H1625-34.

Sims MW, Winter J, Brennan S, Norman RI, André Ng G, Squire IB & Rainbow RD (2014). PKC-mediated toxicity of elevated glucose concentration on cardiomyocyte function. *Am J Physiol Circ Physiol* **307,** H587–H597.

Squire IB, Nelson CP, Ng LL, Jones DR, Woods KL & Lambert PC (2010). Prognostic value of admission blood glucose concentration and diabetes diagnosis on survival after acute myocardial infarction: results from 4702 index cases in routine practice. *Clin Sci (Lond)* **118,** 527–535.

Steg PG et al. (2012). ESC Guidelines for the management of acute myocardial infarction in patients presenting with ST-segment elevation. *Eur Hear J* **33,** 2569–2619.

Su H, Ji L, Xing W, Zhang W, Zhou H, Qian X, Wang X, Gao F, Sun X & Zhang H (2013). Acute hyperglycaemia enhances oxidative stress and aggravates myocardial ischaemia/reperfusion injury: role of thioredoxin-interacting protein. *J Cell Mol Med* **17,** 181–191.

Svensson AM, McGuire DK, Abrahamsson P & Dellborg M (2005). Association between hyper- and hypoglycaemia and 2 year all-cause mortality risk in diabetic patients with acute coronary events. *Eur Hear J* **26,** 1255–1261.

Timmer JR, Hoekstra M, Nijsten MWN, van der Horst ICC, Ottervanger JP, Slingerland RJ, Dambrink J-HE, Bilo HJG, Zijlstra F & van 't Hof AWJ (2011). Prognostic Value of Admission Glycosylated Hemoglobin and Glucose in Nondiabetic Patients With ST-Segment-Elevation Myocardial Infarction Treated With Percutaneous Coronary Intervention. *Circulation* **124,** 704–711.

Weston C, Walker L & Birkhead J (2007). Early impact of insulin treatment on mortality for hyperglycaemic patients without known diabetes who present with an acute coronary syndrome. *Heart* **93,** 1542–1546.

Yang Z, Tian Y, Liu Y, Hennessy S, Kron IL & French BA (2013). Acute hyperglycemia abolishes ischemic preconditioning by inhibiting Akt phosphorylation: normalizing blood glucose before ischemia restores ischemic preconditioning. *Oxid Med Cell Longev* **2013,** 329183.

Yiadom MYAB (2011). Emergency department treatment of acute coronary syndromes. *Emerg Med Clin North Am* **29,** 699–710, v.

Yu Q, Zhou N, Nan Y, Zhang L, Li Y, Hao X, Xiong L, Lau WB, Ma XL, Wang H & Gao F (2014). Effective glycaemic control critically determines insulin cardioprotection against ischaemia/reperfusion injury in anaesthetized dogs. *Cardiovasc Res* **103,** 238–247.

Competing interests.

The authors have no competing interests to declare.

Author Contributions:

All work was carried out at the University of Leicester in RDR's laboratory.

SB: Contributed to experimental design, acquired, analysed and interpreted the data. Drafted and helped revise the manuscript.

SC: Acquired, analysed and interpreted the data and helped with manuscript revision

SM: Acquired, analysed and interpreted the data and helped with manuscript revision

CAM: Acquired, analysed and interpreted the data and helped with manuscript revision

MWS: Acquired, analysed and interpreted the data.

ASAA: Acquired, analysed and interpreted the data

JMW: Acquired, analysed and interpreted the data and revised the manuscript.

IBS: Conception and design of the work and critically appraised and revised the manuscript.

RDR: Conception and design of the work. Acquired, analysed and interpreted the data and critically appraised and revised the manuscript.

Figure 1

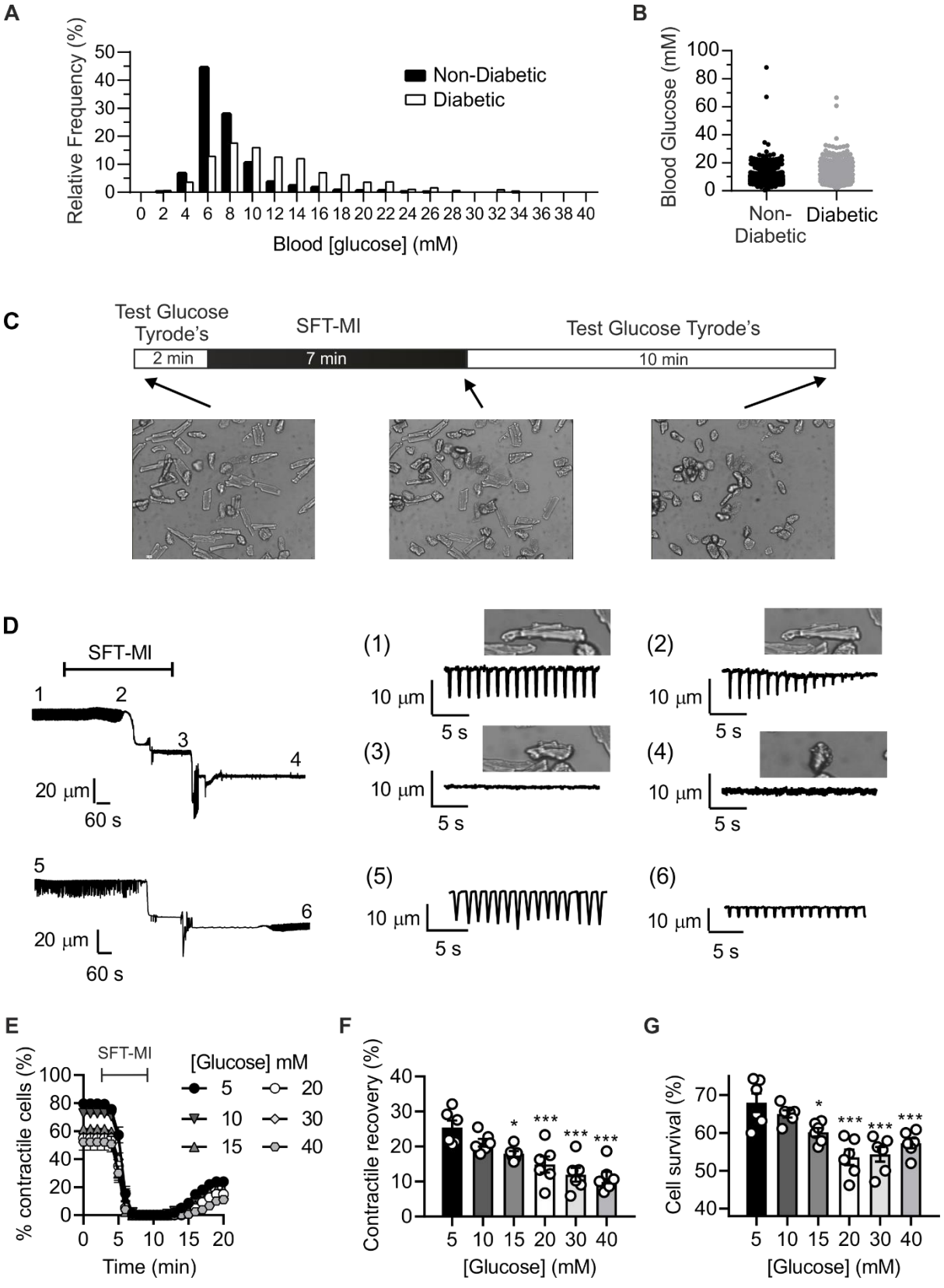
A
Relative Frequency (%)
Non-Diabetic
Diabetic
Blood [glucose] (mM)
B
Blood Glucose (mM)
Non-Diabetic
Diabetic
C
Test Glucose Tyrode's
SFT-MI
Test Glucose Tyrode's
2 min
7 min
10 min
D
SFT-MI
20 μm
60 s
(1)
(2)
(3)
(4)
(5)
(6)
10 μm
5 s
E
SFT-MI
[Glucose] mM
% contractile cells (%)
Time (min)
F
Contractile recovery (%)
[Glucose] (mM)
G
Cell survival (%)
[Glucose] (mM)

Figure 1. Glucose is elevated in AMI patients and augments the cardiotoxic effect of simulated ischaemia and reperfusion in cellular AMI models. Relative frequency histogram (A) and raw values (B) of blood glucose concentration, at the time of admission, in non-diabetic or diabetic AMI patients. (C) SFT-MI protocol showing example photographs of cells prior to metabolic inhibition, at the end of metabolic inhibition and at the end of the reperfusion phase. (D) example recordings to two cells using video edge detection measurements, top trace showing no contractile recovery on reperfusion and the bottom trace showing recovery. To the right are 30 s expanded sections of the trace showing individual contractions as downwards deflections representing the rhythmic shortening of myocytes. Traces and images 1 – 4 show (1) control contraction, (2) contractile failure, (3) end of metabolic inhibition and (4) end of simulated reperfusion. Traces 5 and 6 show (5) control contractions and (6) recovery of contractions in the recovering cell. (E) Time-course showing the percentage of contractile rod-shaped cardiomyocytes during SFT-MI protocol with various glucose concentrations as indicated. Histograms showing percentage contractile recovery (F) and cell survival (G), confirmed by Trypan Blue labelling) after 10 min reperfusion in various glucose concentrations (*P<0.05, ***P<0.001; One-Way ANOVA with Holm-Šídák post-test). n≥91 cardiomyocytes, 6 experiments, ≥3 animals for each data set. Experimental design used shown above the data.

Figure 2

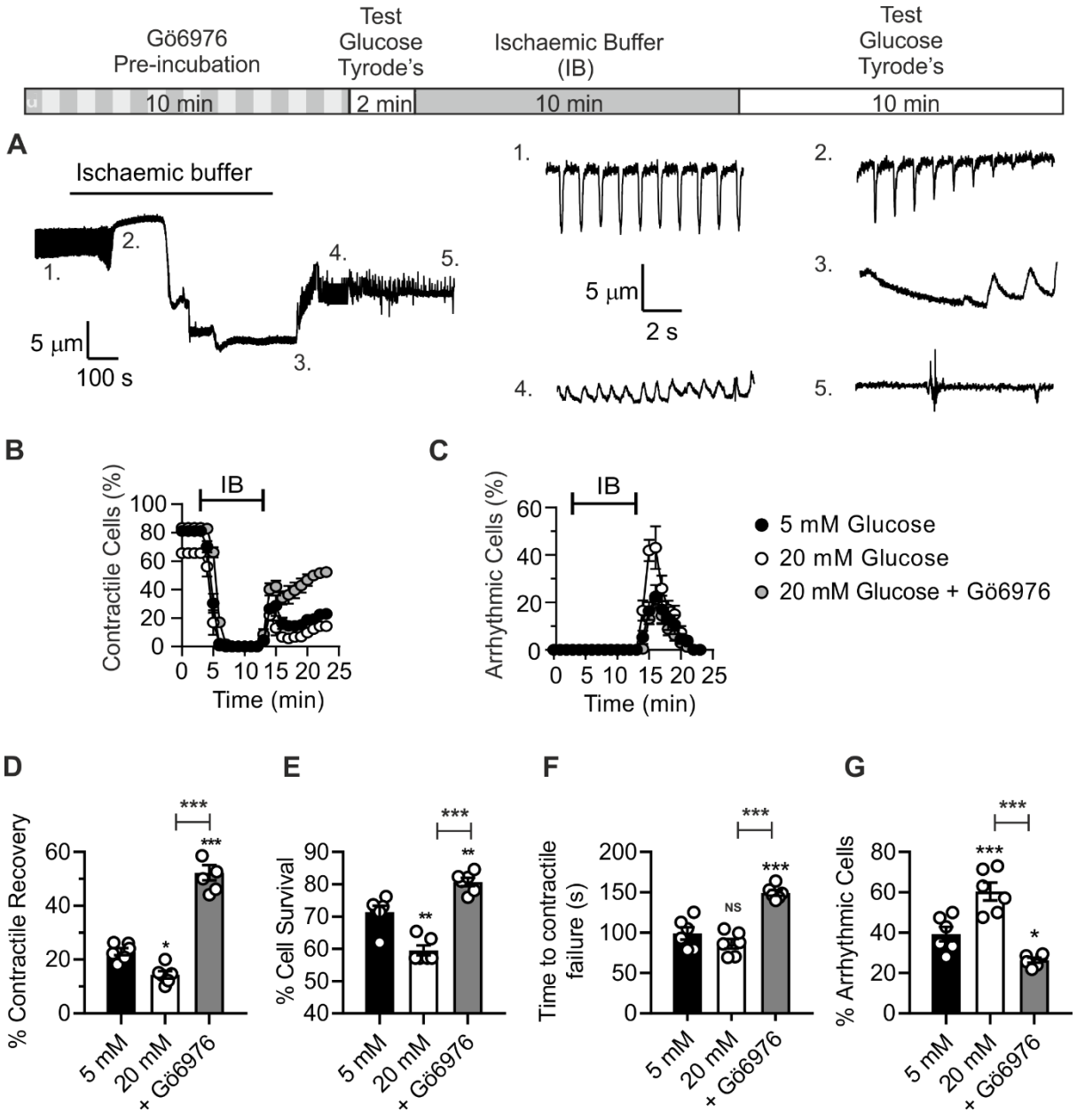

Figure 2: Gö 6976 reveals a glucose dependent cardioprotection against the damage caused by an ischaemic buffer. (A) example video edge detection recording from a single cardiomyocyte exposed to the ischaemic buffer and reperfusion. Expanded traces show 30 s of recording in (1) control conditions, (2) contractile failure, (3) on reperfusion where contraction resumes in all cells, (4) arrhythmias, not synchronous with EFS and (5) cell death (identified by Trypan blue staining. **(**B) Time-course showing the percentage of contractile rod-shaped cardiomyocytes (B) or arrhythmic cells (C) during ischaemic buffer protocol. Three conditions shown are in 5 and 20 mM glucose plus 20 mM glucose after pre-incubation with Gö 6976. Histograms depict percentage contractile recovery (D), Cell Survival (E), the time to contractile failure (F) and percentage arrhythmic cells (G) after the ischaemic

buffer protocol. *P<0.5 **P<0.01, ***P<0.001, One-Way ANOVA with Holm-Šídák post-test. n≥126 cardiomyocytes, 6 experiments, from ≥3 animals for each data set. Experimental design used shown above the data.

Figure 3

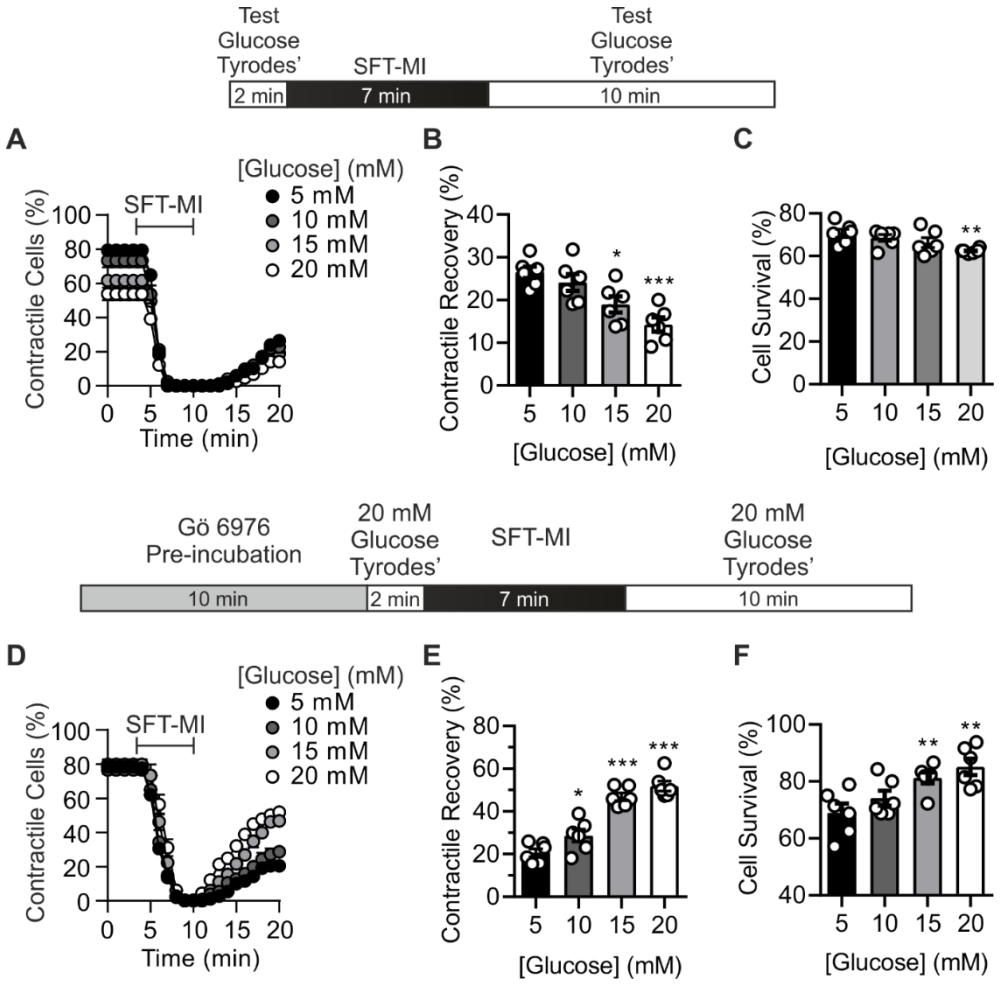

Figure 3: Gö 6976 reveals a glucose-dependent cardioprotection in guinea pig cardiomyocytes. A) Time-course showing the percentage of contractile rod-shaped cardiomyocytes during I/R protocol in various concentrations of glucose. Histograms showing percentage contractile recovery (B) and percentage cell survival (C) after 10 min reperfusion in various glucose concentrations. Graphs D-F show the same data as above but with the addition of a 10 min Gö 6976 pre-incubation period (*P<0.05, **P<0.01, ***P<0.001; One Way ANOVA with Holm-Šídák post-test). n≥90 cardiomyocytes (6 experiments) from ≥3 animals for each data set. Experimental design used shown above each data set.

Figure 4

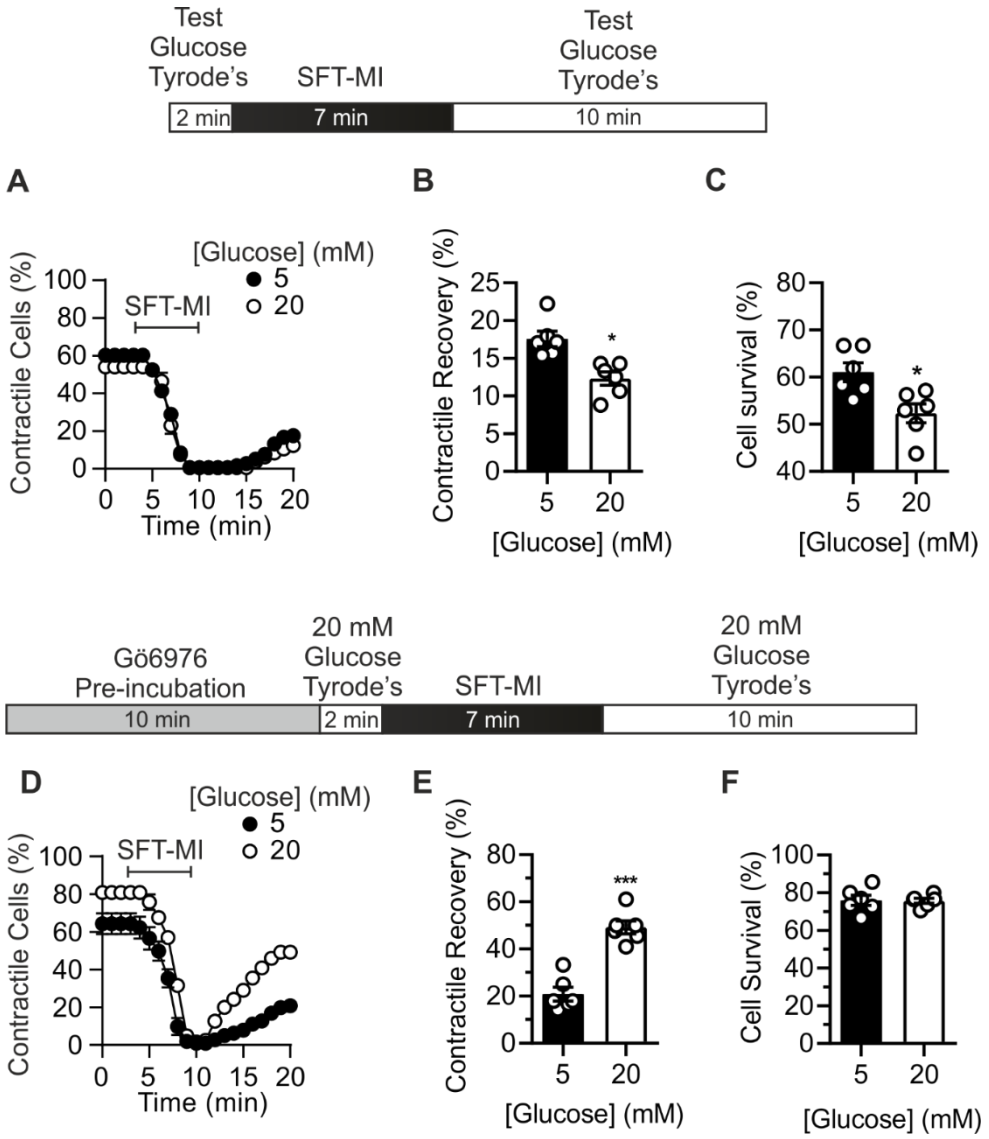

Figure 4: Gö 6976 reveals a glucose-dependent cardioprotection in rabbit cardiomyocytes. A) Time-course showing the percentage of contractile rod-shaped cardiomyocytes during I/R protocol in 5 or 20 mM glucose. Histograms showing percentage contractile recovery (B) and percentage cell survival (C) after 10 min reperfusion in 5 or 20 mM glucose. Graphs D-F show the same data as above but with the addition of a 10 min Gö 6976 pre-incubation period (*P<0.05, **P<0.01, ***P<0.001; Unpaired T-test). n≥83 cardiomyocytes (6 experiments) from ≥3 animals for each data set. Experimental design used shown above each data set.

Figure 5

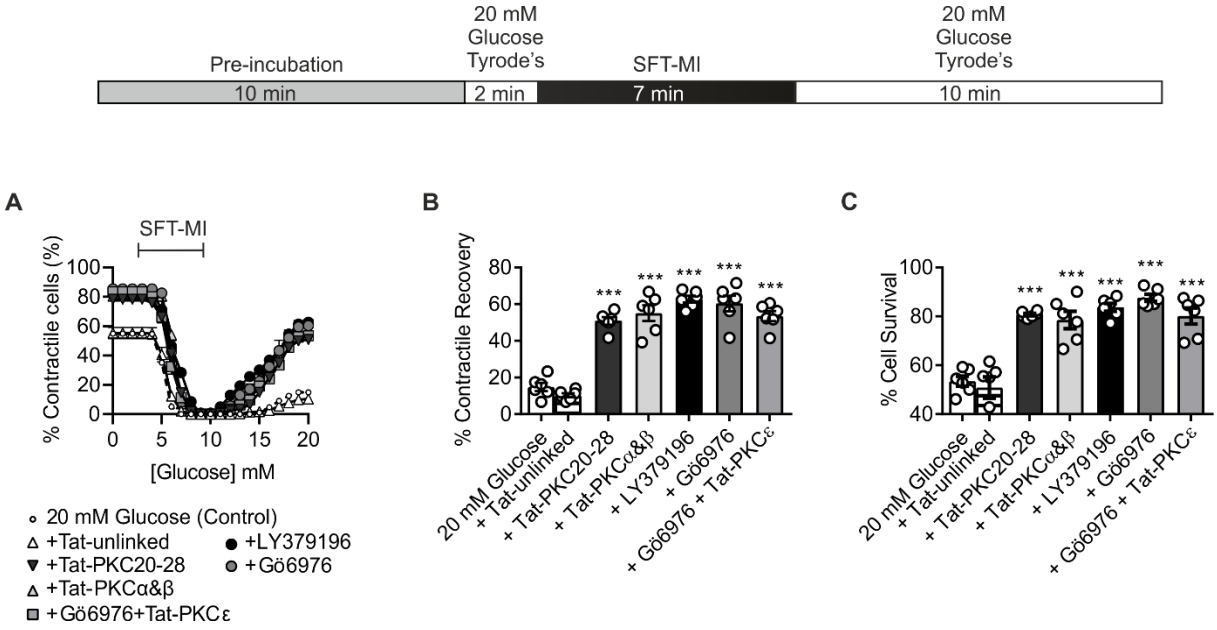

Figure 5. PKCα/β inhibition reveals a glucose-dependent cardioprotective mechanism. A) Time-course showing the percentage of contractile rod-shaped cardiomyocytes during SFT-MI protocol in 20G (control) and with pre-incubation of the inhibitors as indicated in figure. Histograms depict percentage contractile recovery (B) and cell survival (C) after SFT-MI in 20G or with pre-incubation of the inhibitors (***P<0.001, One-Way ANOVA with Holm-Šídák post-test). n≥82 cardiomyocytes, ≥5 experiments, ≥3 animals for each data set. Experimental design used shown above the data.

Figure 6

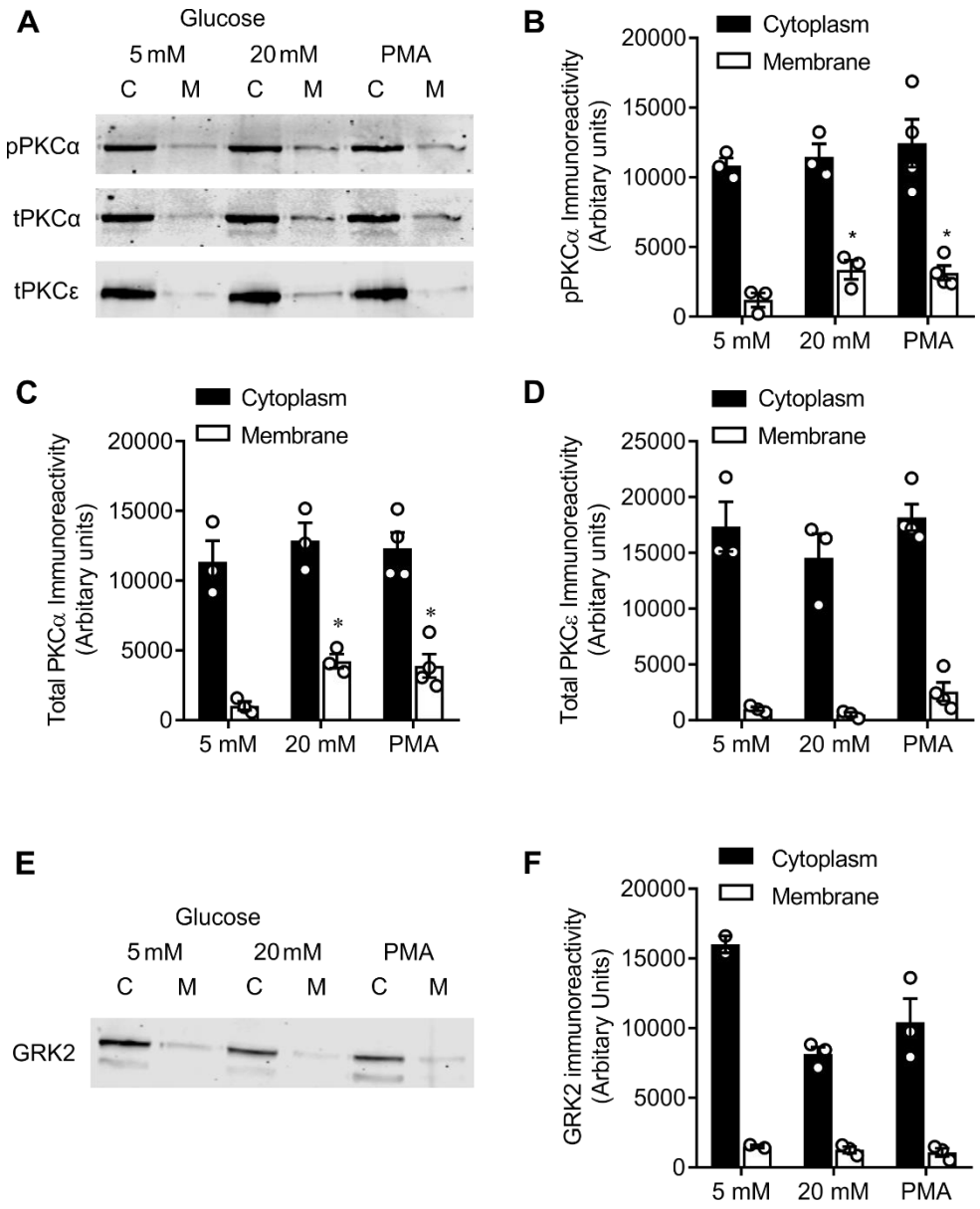

Figure 6: High glucose treatment causes increased PKCα recruitment to cardiomyocyte membranes. Hearts were treated with 5 or 20 mM glucose or PMA (1 μM) for 30 min. After treatment tissues were homogenised and separated into cytosolic and membrane factions. Lyates were subjected to SDS-PAGE separation and probed for phospho-PKCα total PKCα and total PKCε. Representative immunoblots (A) and cumulative data (means ± SEM; for n = ≥3 hearts per treatment) show the effects of glucose and PMA on the cellular distribution of phospho-PKCα (B), total PKCα (C) and PKCε (D). High glucose (20 mM) and PMA increased the recruitment of PKCα and phosphor PKCα to the membrane fraction but not PKCε (*p<0.05; one-way ANOVA, Dunnett's *post hoc* test). Lysates were

also probed for GRK2 expression. Representative immunoblot (A) and cumulative data (B) (means ± SEM; for n = ≥3 hearts per treatment) show the effects of glucose and PMA on the cellular distribution of GRK2. High glucose (20 mM) does not promote GRK2 recruitment to the membrane fraction.

Figure 7

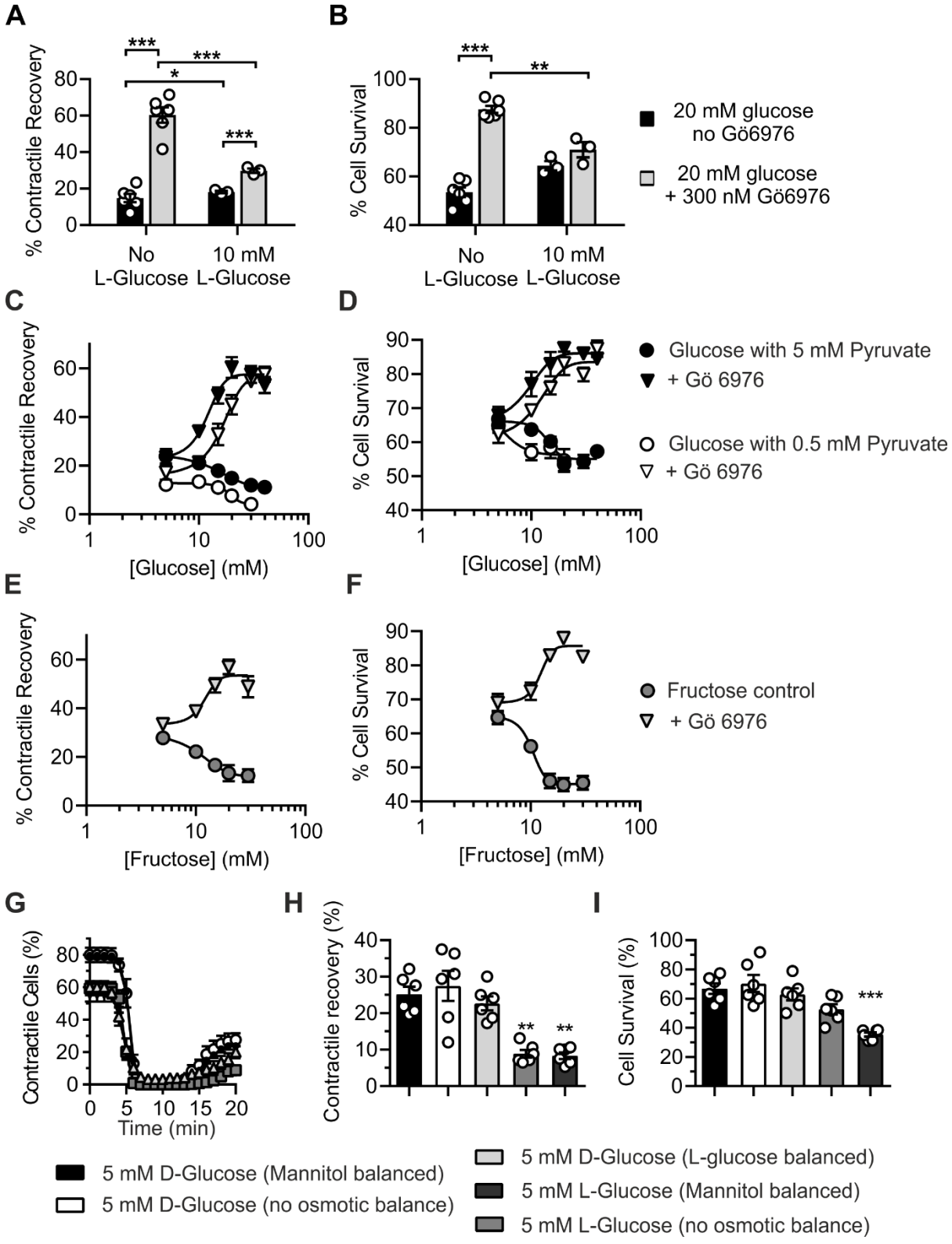
A
B
% Contractile Recovery
% Cell Survival
No L-Glucose
10 mM L-Glucose
20 mM glucose no Gö6976
20 mM glucose + 300 nM Gö6976
C
D
[Glucose] (mM)
Glucose with 5 mM Pyruvate
+ Gö 6976
Glucose with 0.5 mM Pyruvate
+ Gö 6976
E
F
[Fructose] (mM)
Fructose control
+ Gö 6976
G
H
I
Contractile Cells (%)
Time (min)
Contractile recovery (%)
Cell Survival (%)
5 mM D-Glucose (Mannitol balanced)
5 mM D-Glucose (no osmotic balance)
5 mM D-Glucose (L-glucose balanced)
5 mM L-Glucose (Mannitol balanced)
5 mM L-Glucose (no osmotic balance)

Figure 7: Gö 6976 imparts cardioprotection via a metabolism dependent pathway. Histograms depict percentage contractile recovery (A) and cell survival (B) after SFT-MI in 20G in the presence or absence of 300nM Gö6976 with or without 10mM L-glucose (*P<0.05, **p=P<0.01, ***P<0.001, Two-Way ANOVA with Holm-Šídák post-test). n≥87 cardiomyocytes, >3 experiments, ≥3 animals for each data set. Concentration-response curves showing percentage contractile recovery (C) and percentage cell death (D) with increasing glucose + 5 or 0.5 mM pyruvate in the absence (circles) or presence (triangles) of 300 nM Go 6976. Concentration-response curves showing percentage contractile recovery (E) and percentage cell death (F) with increasing fructose with 5 mM pyruvate in the absence (circles) or presence (triangles) of 300 nM Go 6976. The line on each graph represents the Hill equation fit to the data. n≥86 cardiomyocytes (6 experiments) from ≥3 animals for each data set. (G) Time-course showing the percentage of contractile rod-shaped cardiomyocytes during I/R protocol in various conditions including metabolizable and non- metabolizable sugars. Histograms showing percentage contractile recovery (H) and percentage cell survival (I) after 10 min reperfusion in the various conditions tested (**P<0.01, ***P<0.001; One Way ANOVA with Holm-Šídák post-test). n≥111 cardiomyocytes, 6 experiments from ≥3 animals for each data set. Experimental design used shown above each data set.

Figure 8

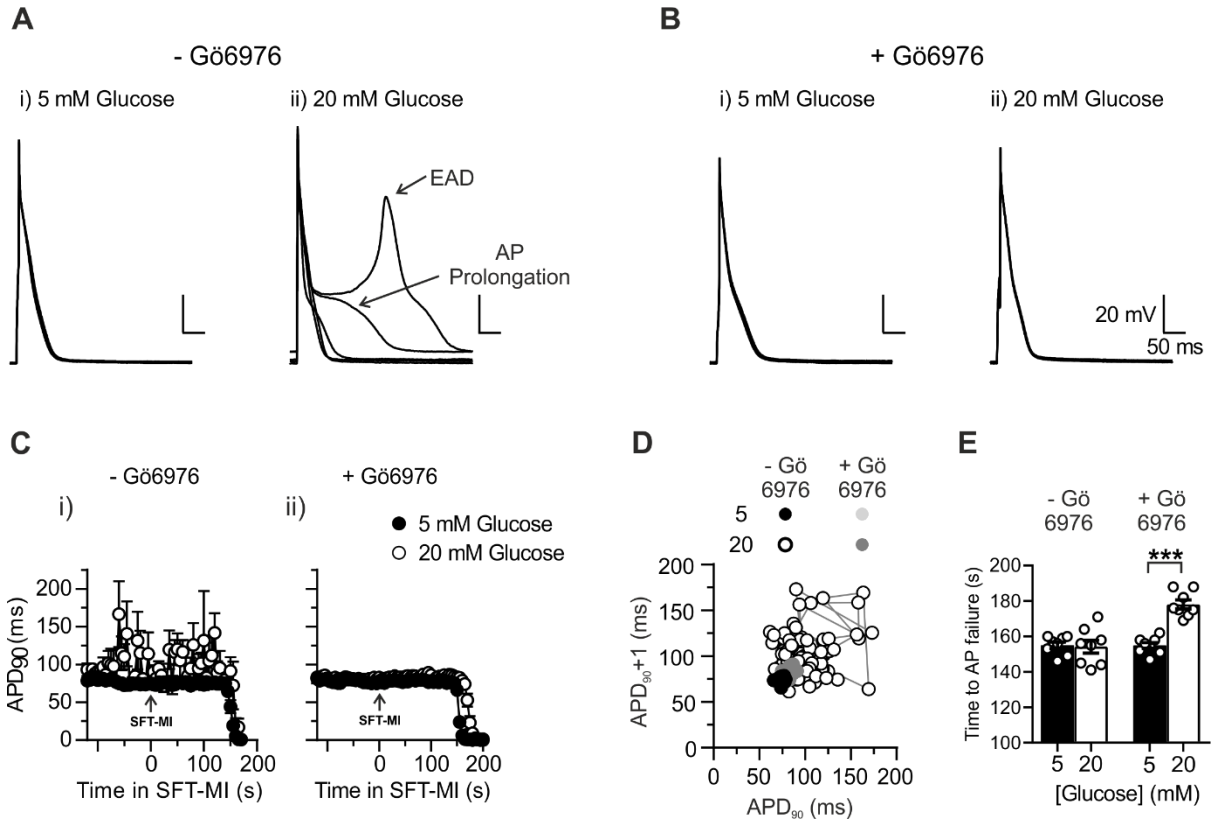

Figure 8: Glucose-induced perturbation in electrical signalling during simulated ischaemia in rat cardiomyocytes is attenuated by Gö6976. Example action potentials during simulated ischaemia recorded from rat cardiomyocytes in 5G (Ai) and 20G (Aii) without and with Gö6976 (Bi-ii). C) Mean change in AP duration to 90% repolarization (APD_{90}) after perfusion in 5G or 20G without (i) and with (ii) 300 nM Gö6976. Arrows indicate time=0, the point at which SFT-MI was perfused on to cardiomyocytes. D) Poincaré plot showing the average APD_{90} for the first 120 APs during SFT-MI in the four conditions. E) Mean time to AP failure in SMT-MI in the four conditions (***P<0.001 Two-Way ANOVA with Holm-Šídák post-test). n≥8 cardiomyocytes, ≥3 animals for each data set.

Figure 9

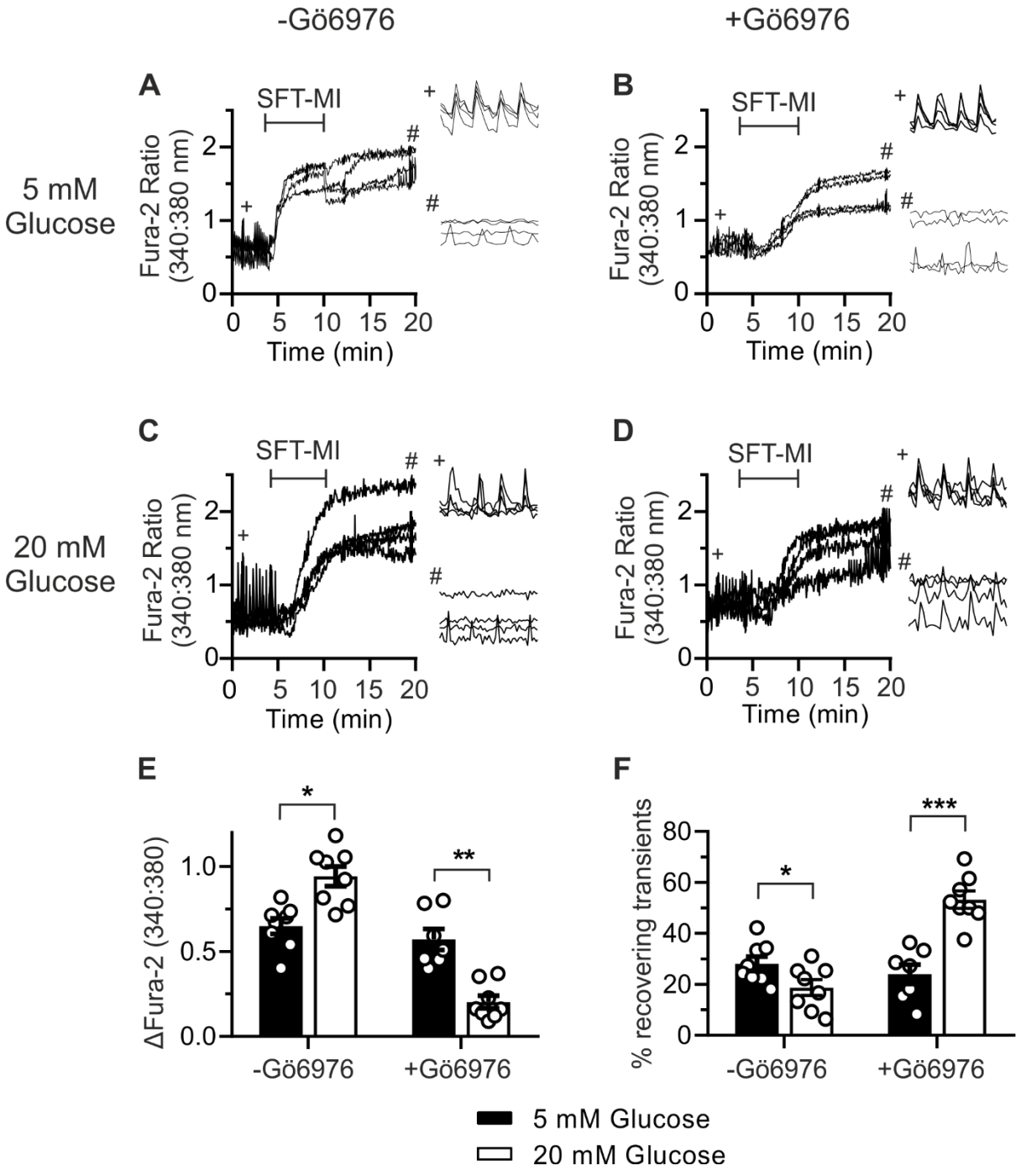

Figure 9: Gö6976 attenuates the glucose-mediated deleterious effects of intracellular calcium accumulation in rat cardiomyocytes during simulated ischaemia. Time-courses showing the Fura-2 ratio during SFT-MI protocol in 5G or 20G without (-) and with (+) Gö6976 (A-D). Cells were stimulated to contract by EFS throughout the protocol. Ca^{2+} transients were recorded at the beginning (+) and end (#) of the recording and were recorded at a rate of 12 Fura-2 ratios s^{-1} (24 fps). For the rest

of the protocol, data was acquired at 0.2 Hz. E) Mean change in Fura-2 ratio before and after SFT-MI for 5G or 20G without (-) and with (+) Gö6976. F) Mean percentage of cells recovering transients at the end of the SFT-MI protocol for 5G and 20G without (-) and with (+) Gö 6976**.** (*P<0.05, **P<0.01, ***P<0.001 Two-Way ANOVA with Holm-Šídák post-test). n≥87, ≥6 experiments, ≥3 animals for each data set.

Figure 10

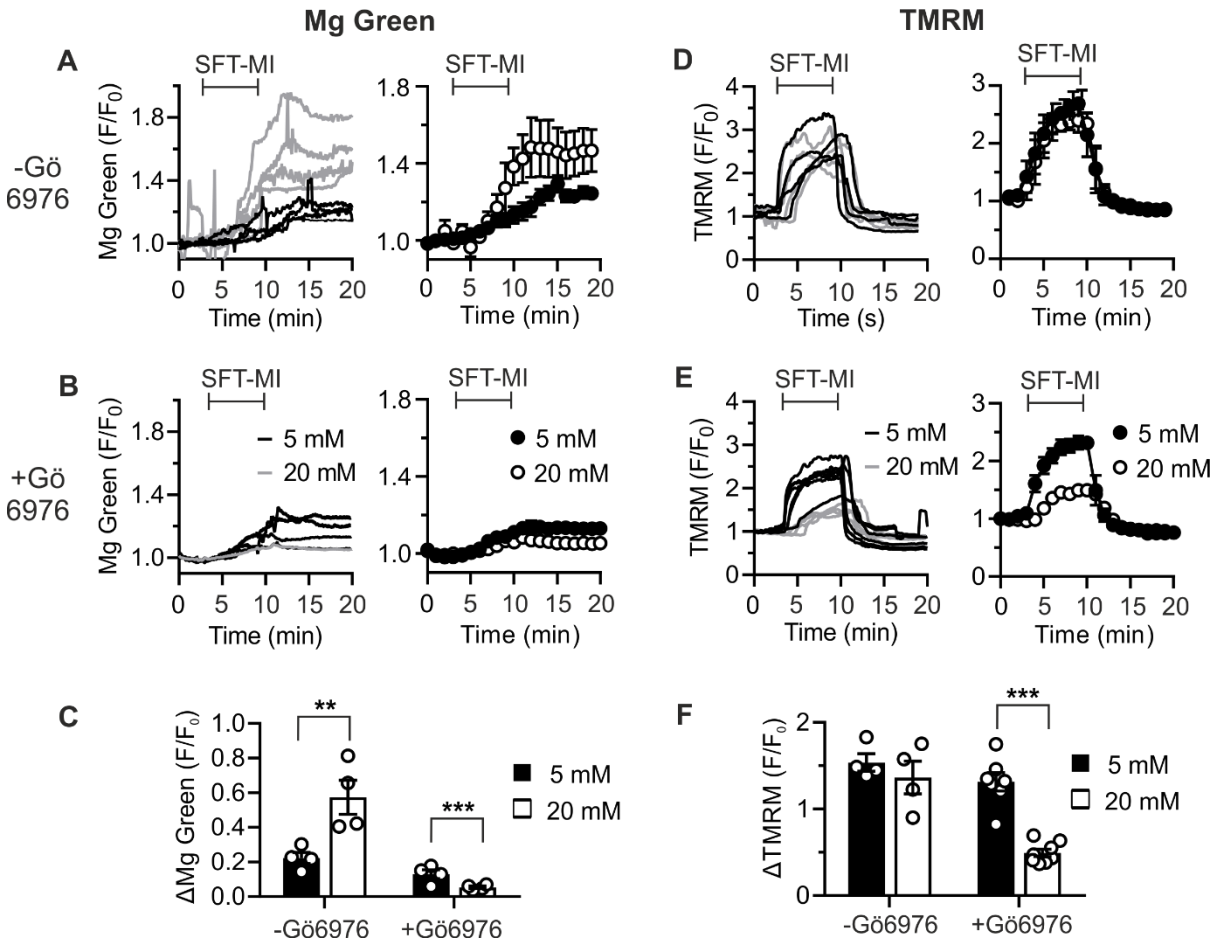

Figure 10: Fluorescent imaging with MgGreen and TMRM shows that Gö6976 attenuates the effect of 20G on ATP production and mitochondrial membrane potential in simulated ischaemia. Time-courses showing the MgGreen fluorescence (F/F0) from 4 cells, and mean data from 4 experiments, throughout the SFT-MI protocol in 5G and 20G without (-; A) and with (+; B) Gö6976. C) Mean change in MgGreen fluorescence at the end of SFT-phase for 5G and 20G without (-) and with (+) Gö6976. (**P<0.01, ***P<0.001, Two-Way ANOVA with Holm-Šídák post-test). n≥29 cardiomyocytes, ≥4 experiments from ≥4 animals for each data set. Time-courses showing the TMRM fluorescence (F/F0) from 4 cells, and mean data from 4 experiments, throughout the SFT-MI protocol in 5G and 20G without (-; D) and with (+; E) Gö6976. F) Mean change in TMRM fluorescence at the end of SFT-phase for 5G and 20G without (-) and with (+) Gö6976 (***P<0.001, Two-Way ANOVA with Holm-Šídák post-test). n≥41 cardiomyocytes, ≥4 experiments from ≥4 animals for each data set. Experimental design as shown in Figure 1.

Figure 11

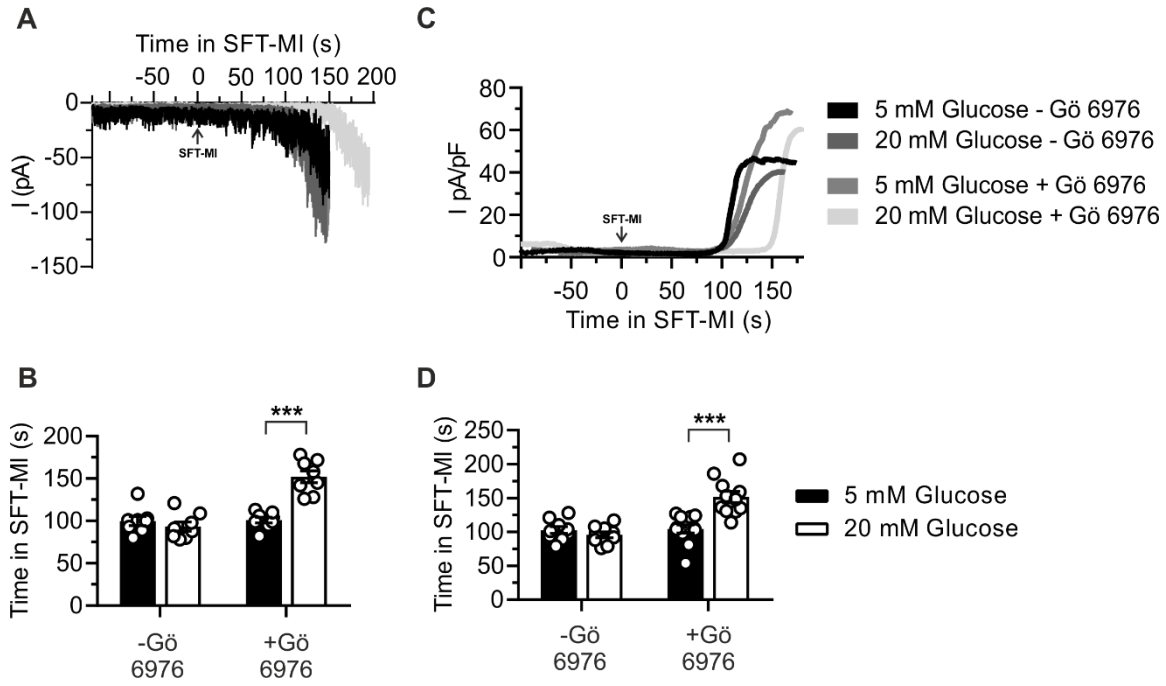

Figure 11: Time to K_{ATP} channel opening and development of a metabolically-sensitive leak-current are delayed by Gö6976 in the presence elevated glucose. A) Example traces of cell-attached patch recording of rat cardiomyocytes showing the time to K_{ATP} channel opening during SFT-MI following 5 or 20 mM glucose in the absence and presence of Gö6976. B) Mean time to K_{ATP} channel opening during SFT-MI perfusion in all 4 conditions. C) Example traces of whole-cell patch recording displaying the leak current activated during SFT-MI perfusion in 5 and 20 mM glucose in the absence and presence of Gö6976. D) Mean time to increase in leak current during SFT-MI perfusion in all 4 conditions (***P<0.001, Two-Way ANOVA with Holm-Šídák post-test). n≥8 cardiomyocytes, ≥8experiments, ≥3 animals for each data set. Arrows indicate time=0, the point at which SMT-MI was perfused on to cardiomyocytes.

Figure 12

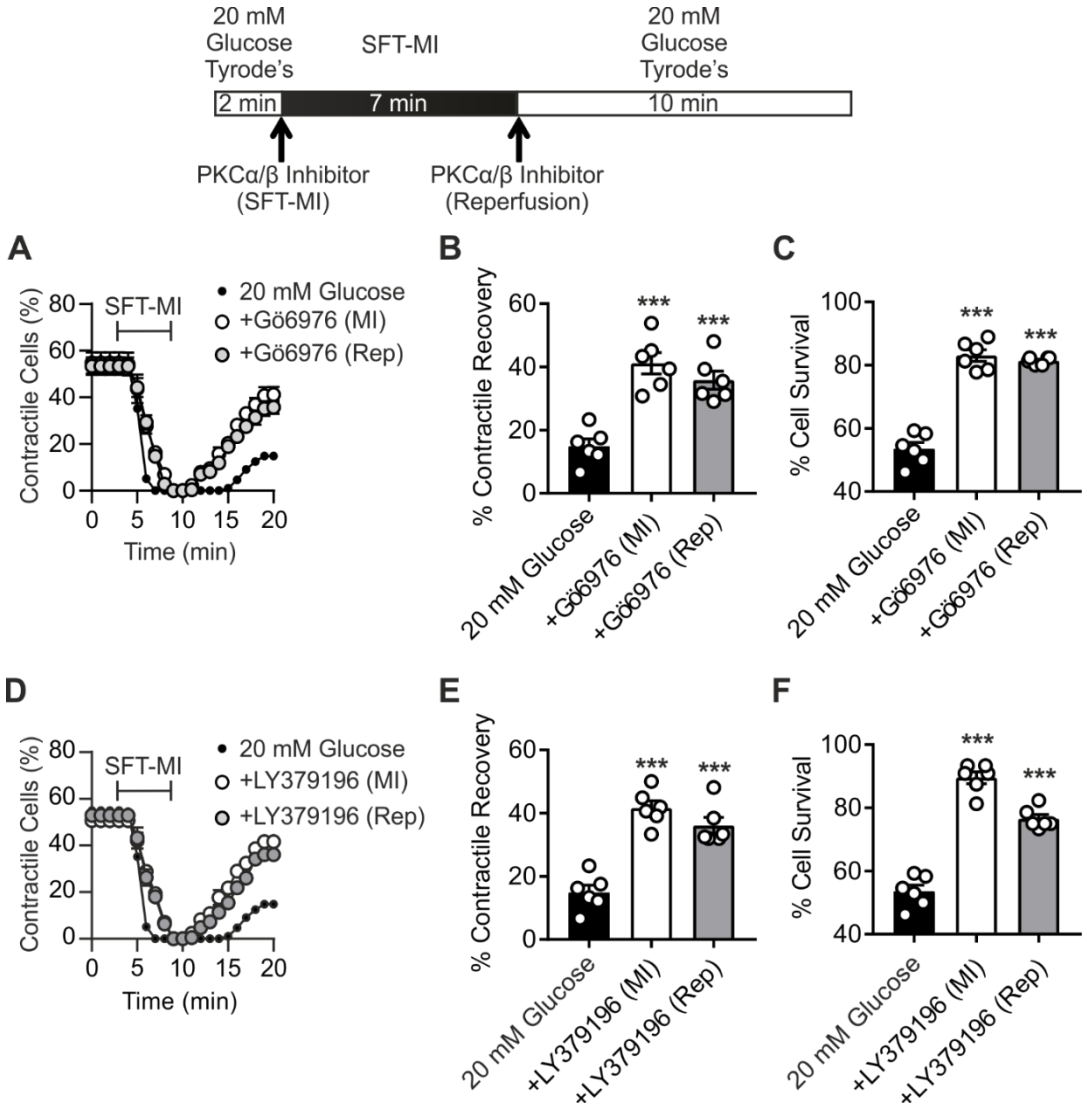

Figure 12: Gö6976 and LY379196 impart cardioprotection when applied before simulated ischaemia or reperfusion. A) Time-course showing the percentage of contractile cardiomyocytes during SFT-MI protocol in the absence and presence of Gö6976 at the start of simulated ischaemia and reperfusion. Histograms showing percentage contractile recovery (B) and cell survival (C) after 10 min reperfusion in the absence and presence of Gö6976 at the time of simulated ischaemia and reperfusion. Graphs D-F show the results for LY379196. ***P<0.001, One-Way ANOVA with Holm-Šídák post-test. n≥84 cardiomyocytes (6 experiments) from ≥3 animals for each data set. Experimental design used shown above the data.

Figure 13

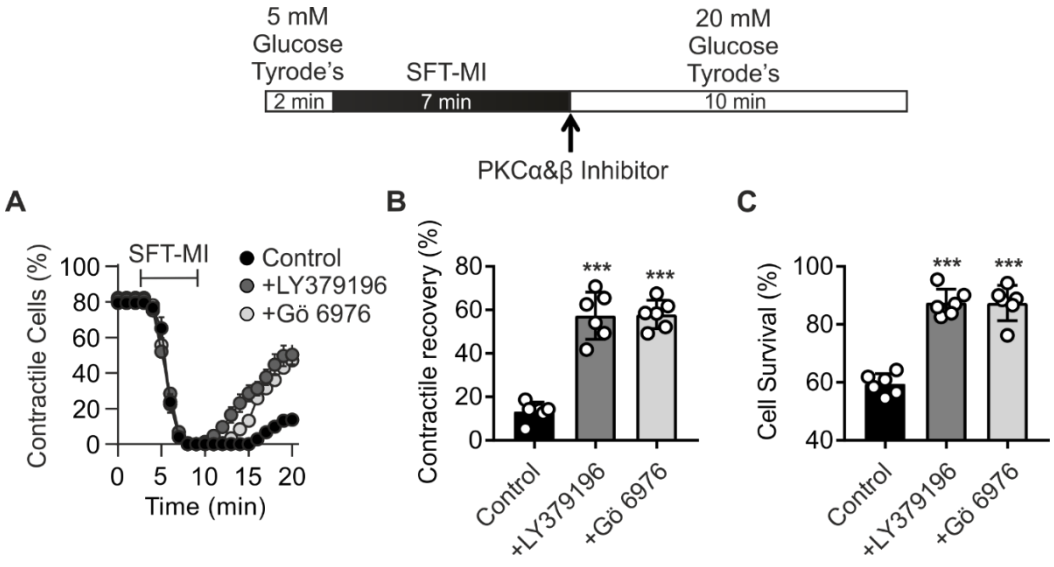

Figure 13: Gö 6976 and LY 379196 impart cardioprotection from the deleterious effects of elevated glucose at reperfusion. A) Time-course showing the percentage of contractile cardiomyocytes during I/R protocol with Gö 6976 or LY 379196 added at reperfusion in elevated glucose. Histograms showing percentage contractile recovery (B) and percentage cell survival after 10 min reperfusion. n≥115 cardiomyocytes, n≥5 experiments n=3 animals for each data set. ***P<0.001, One-Way ANOVA with Holm-Šídák post-test. n≥74 cardiomyocytes (6 experiments) from ≥3 animals for each data set. Experimental design used shown above the data.

Figure 14

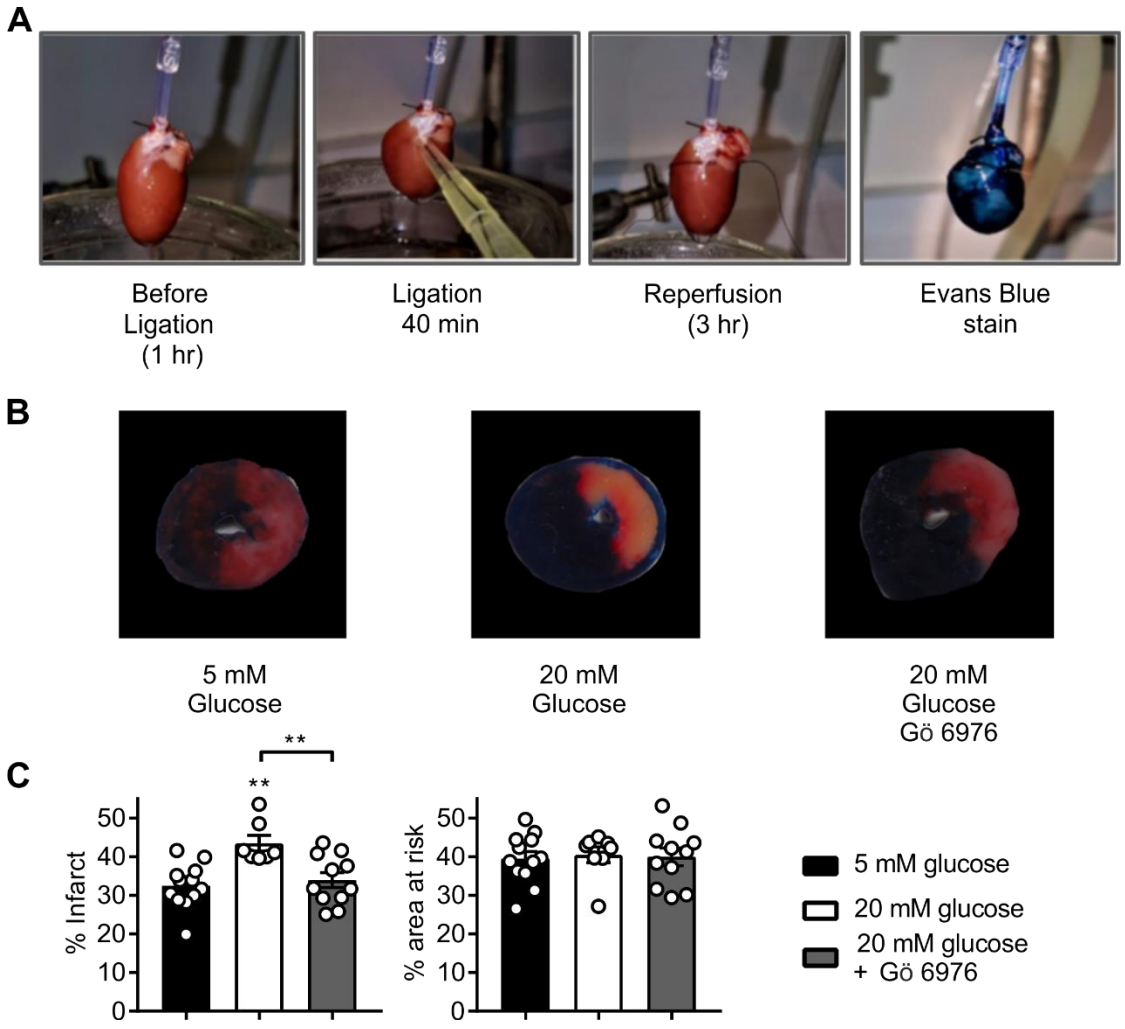

Figure 14: Gö6976 imparts cardioprotection against glucose induced damage during whole heart coronary ligation. A) representative pictures showing the whole heart (from left to right) before and during ligation, reperfusion and Blue Evans staining. B) Representative sections for each condition showing the infract size as measured by of TTC staining (white), area at risk (red) and unaffected area (Blue). C) Histograms depict infarct as a percentage of the area at risk (Left) and percentage area at risk of the whole heart (Right) in each condition as a control for experimental variability. **P<0.01, OneWay ANOVA with Holm-Šídák post-test. n = 8 hearts for each group.

Figure 15

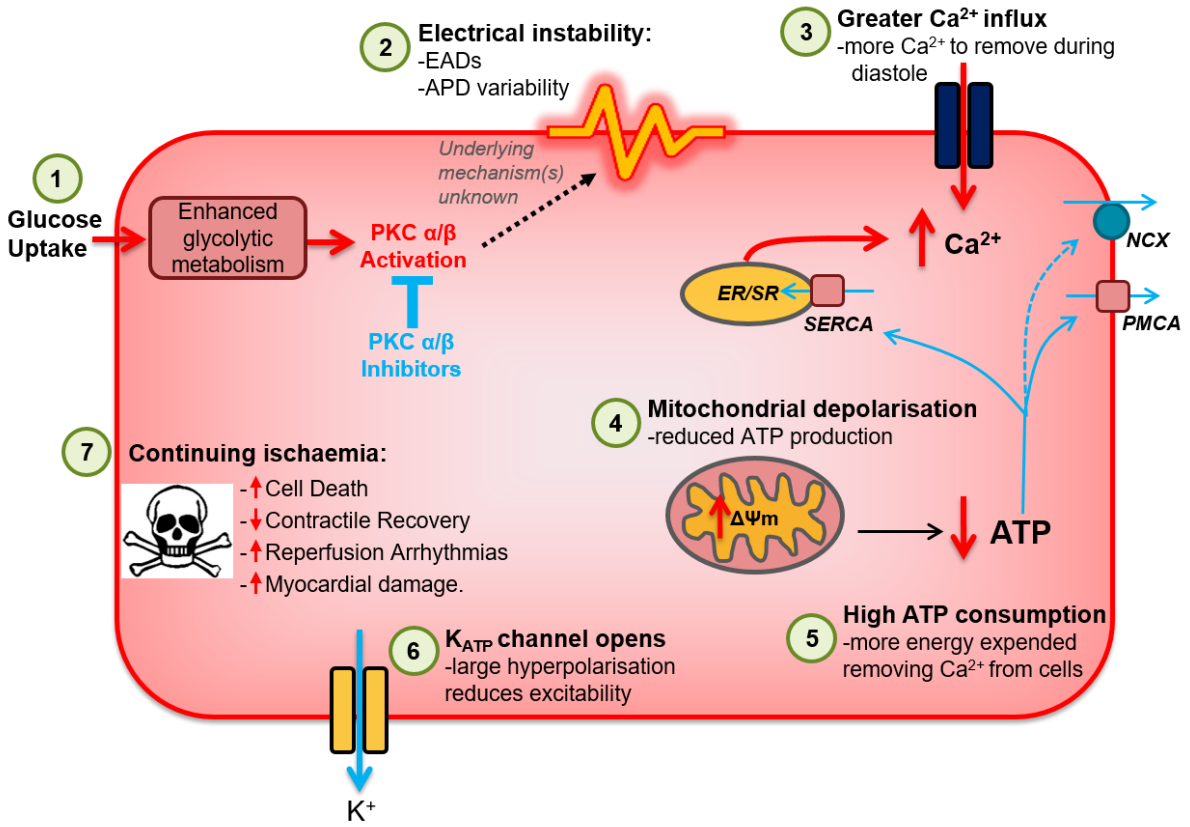

Figure 15: The proposed mechanism of glycaemia-PKCα/β inhibition dependent cardioprotection against simulated ischaemia. 1) The underlying molecular mechanism(s) linking glucose-glycolytic metabolism-PKCα/β activation with myocardial damage remain unclear. 2) Enhanced glycolytic metabolism-PKCα/β activation caused early after depolarisations (EADs) and action potential duration (APD) variability. 3) Electrical instability resulted in a greater influx of Ca^{2+} into the cells. 4) Prolonged ischaemia will result in mitochondrial depolarisation (ΔΨm) and so reduce ATP production. 5) In turn Ca^{2+} accumulates as there is not enough ATP to drive removal of Ca^{2+} via SERCA, PMCA or indirectly by NCX. 6) If ATP levels decrease sufficiently, the cardiac K_{ATP} channel activates and produce a large hyperpolarisation to reduce cell excitability. 7) As ischaemia conditions continue, enhanced glycolytic metabolism-PKCα/β activation increase in myocardial damage and reperfusion arrhythmias. The presence of PKCα/β inhibitors in high glucose preserved electrical function, reduced Ca^{2+} accumulation and so ATP consumption, whilst preserving mitochondrial membrane potential so ATP production. K_{ATP} activation was delayed, a marker of delayed ATP depletion, and the functional recovery was

improved on reperfusion. The colour red has been used to indicate potentially toxic changes with elevated glucose whilst blue indicates potentially protective mechanisms.